



Cite this: *Biomater. Sci.*, 2026, **14**, 81

## Catechol modification as a platform for functional coatings

Banibrata Maiti, <sup>a</sup> Erik V. Van der Eycken <sup>a,b</sup> and Guglielmo A. Coppola <sup>\*a</sup>

Catechol-based surface functionalization has emerged as a powerful strategy for tailoring material properties and enabling diverse applications, owing to its robust adhesive capabilities and broad substrate compatibility. Inspired by mussel foot proteins and popularized by dopamine-derived polydopamine coatings, catechol grafting has evolved into a versatile platform for anchoring molecules of interest (MOI) onto surfaces. This review focuses on the synthetic strategies for direct covalent modification of active compounds—such as polymers, peptides, and small molecules—with catechol moieties, bypassing the limitations of traditional bottom-up and co-deposition approaches. By examining the reactivity profiles of catechol precursors and their coupling chemistries, we aim to provide a comprehensive framework for designing functional coatings with enhanced performance and simplified processing. This work fills a critical gap in the literature by offering practical guidelines for researchers seeking to harness catechol chemistry in advanced material engineering.

Received 9th September 2025,  
Accepted 14th November 2025

DOI: 10.1039/d5bm01363a  
[rsc.li/biomaterials-science](http://rsc.li/biomaterials-science)

## Introduction

Surface functionalization offers appealing solutions to fine-tune material characteristics or confer new properties (e.g. anticorrosion, self-cleaning or bioactivity).<sup>1,2</sup> Abundant litera-

ture has been produced covering a variety of coating strategies towards a plethora of application fields. The success of a coating procedure can be largely ascribed to its versatility, reproducibility and ease of application. In this frame catechol grafting gained great success especially in light of the virtually material-agnostic adhesive properties. The seminal paper by Messersmith *et al.* on the preparation of thin coatings with dopamine, brought widespread popularity to catechol grafting.<sup>3</sup> This concept sprouted from previous studies on mussels foot proteins (Mfps) adhesive properties which resulted in plural and intensive efforts towards the elucidation of the

<sup>a</sup>Laboratory for Organic & Microwave-Assisted Chemistry (LOMAC), Department of Chemistry, KU Leuven, Celestijnenlaan 200F, B-3001 Leuven, Belgium.

E-mail: guglielmo.coppola@kuleuven.be

<sup>b</sup>Peoples' Friendship University of Russia (RUDN University), Miklukho-Maklaya Street 6, Moscow, 117198, Russia



Banibrata Maiti

Banibrata Maiti received his master's degree in chemistry from the Indian Institute of Technology Kanpur, India in 2022. He is currently pursuing his PhD under the supervision of Prof. Dr Erik Van der Eycken at KU Leuven. His research interests focus on synthesising bioactive heterocycles and developing anti-bacterial coatings.



Erik V. Van der Eycken

Erik V. Van der Eycken is Full Prof. of Organic Chemistry and Head of the Division of Molecular Design & Synthesis at KU Leuven, Belgium. He received his PhD degree (1987) in organic chemistry from the University of Ghent, Belgium. He spent time as a visiting scientist at the University of Graz (2002) with Prof. C. O. Kappe, at The Scripps Research Institute (La Jolla, USA) (2003) in the group of K. B. Sharpless, and at Uppsala University (2004) with Prof. M. Larhed and Prof. A. Hallberg. His main research focus is on the development of new synthetic methodologies in combination with enabling techniques.



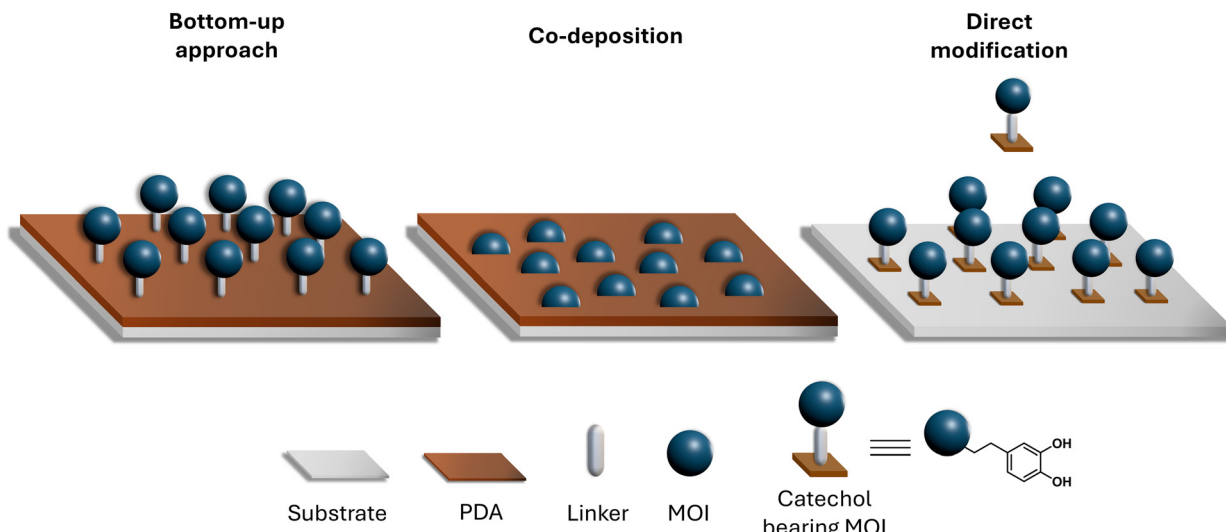


Fig. 1 Graphical representation of the catechol grafting approaches.

molecular mechanism.<sup>4–11</sup> Isolation and characterization of the distal aminoacidic sequences of Mfps showed the presence of alternating of levodopa and lysine (or histidine) sequences and therefore an alternance of catechol and amino groups. This arrangement was individuated as responsible for the extraordinary adhesive properties, further proved by the discovery that L-DOPA could exert similar behavior. Since then, this strategy has proven to be a versatile tool for surface functionalization. The afore mentioned work from Messersmith's group presented dopamine as simplification, reduced to the simplest terms, of the mussels foot proteins adhesive mechanism. Dopamine, containing both a catechol and an amino group, could polymerize in an alkaline oxidative environment to form a thin coating of polydopamine (PDA) on various surfaces. Several works followed exploring the possibility to exploit this new surface chemistry tool for the preparation of functional coatings. The mild reaction conditions in

water-based solvents, together with a virtually complete substrate compatibility (*i.e.* glass, metal, and plastic), granted its successful adoption in a variety of applications, including anticorrosion and antifouling coatings, drug delivery and other biomedical applications. In here we will focus on the use of catechol chemistry for the installation of molecules of interest (MOI), as small molecules and polymers, or reactive functional groups onto target surfaces.

Three different coating approaches can be individuated, *i.e.* (1) bottom-up approach, (2) co-deposition with dopamine, and (3) direct modification of catecholamines or analogues (Fig. 1). Bottom-up coating approaches mostly rely on polydopamine as primer layer for the adhesion of a secondary layer of active molecules. These involve multi-step procedures that end with the formation of a bond between the desired molecule and the pre-formed coating. In some cases, addition of linkers or sequential functional groups insertion/activation is required. Otherwise, when the target molecule presents with the necessary functional groups (amine, thiol), it can react directly with the polydopamine coating. In the co-deposition approach, active molecules covalently bind with the forming PDA polymer or get trapped inside the coating layers. Finally, in direct modification approaches, catechol moieties are added to polymers or small molecules structure to confer adhesive properties.

The application of bottom-up syntheses is limited as multi-step procedures are time-consuming and can present challenges in real-life scenarios in terms of reproducibility and scale-up. Moreover, nonquantitative conversion can result in a dramatic reduction in loading as the number of required steps increases. At the other end of the spectrum, co-deposition is a one-step coating process and usually does not require prior functionalization of the active molecule, neither special optimization of the coating procedure. Nonetheless, this approach offers minimal to no control over the adherence of active molecules to the coating. This can lead to poor surfaces loading of the active compounds and leaves limited room for optimiz-



Guglielmo A. Coppola received his Master's degree in Pharmaceutical Chemistry and Technology (2017) from Sapienza University of Rome. Later in the same year, he joined LOMAC through an Erasmus+ scholarship working on metal-free spirocyclizations. He obtained his PhD in 2022 on the development of antibiofilm coatings, under the supervision of Prof. Erik Van der Eycken and Prof. Hans Steenackers at KU Leuven. His research focuses on antibiofilm strategies and functional coatings for implantable devices.

Guglielmo A. Coppola

Leuven. His research focuses on antibiofilm strategies and functional coatings for implantable devices.



ation. In both aforementioned strategies, polydopamine, or its analogues, constitutes the main component of the coating acting as the adhesive layer.

Contrarily, in direct modification, an active molecule or polymer becomes able to form a film on the surface in a single coating step through the introduction of catechol moieties. This approach has been described soon after the elucidation of Mfps adherence mechanism and before the first reports on polydopamine, by coupling L-DOPA with a polyethylene glycol chain. The procedural simplicity is appealing in terms of ease and cost of production. Moreover, the direct attachment of the desired molecules can result in better surface coverage and higher loadings.

The literature covering the several aspects of polydopamine coating and catechol grafting, spanning from mechanistic investigation, coating preparation, and practical application has been already summarized in the past by other authors.<sup>3,12–14</sup> In 2019, Asha *et al.* reviewed the incorporation of dopamine in zwitterion-conjugated polymers for non-fouling surface engineering.<sup>15</sup> In a 2020 review, Zhang *et al.* discussed the design principles and applications of mussel-inspired hydrogels.<sup>16</sup> Other review articles examined the role of dopamine as a crosslinker and its conjugation with biopolymers such as chitosan, hyaluronic acid, and gelatin.<sup>17</sup> These papers collectively described various approaches for developing dopamine-modified polymers for a wide range of applications. Focusing on the use of direct modification for surface coating a comprehensive description is still missing. The available reports on the synthetic strategies for the installation of catechol moieties on active molecules and polymers are scattered in the literature and suffer from low consistency. This gap hampers the identification of catechol direct modification as an emerging field. A dedicated overview will thus help outlining the scope and limitations of such approach while highlighting its features.

The present work will cover the main catechol precursor molecules (dopamine, levodopa, and other derivatives) exploited in direct modification strategies. These are characterized by different reactivities and offer alternative coupling possibilities (*e.g.* amide bonds, click chemistry) allowing for the design of synthetic strategies tailored to the target molecules. In this article, we will discuss the opportunities, advantages, and limitations which can direct the choice of catechol precursor molecules to transfer adhesive properties to compounds of interest. In here, we specifically focus on the synthetic strategies for the incorporation of catechol moieties into polymers, peptides or small molecules, and the relevant applications in functional coatings and materials. The aim of this review is to provide guidelines for further research in the field of catechol grafting *via* direct modification.

## Catechol precursor and coupling strategy

Catechol moieties are present in a plethora of natural compounds including dopamine and its analogues offering a

variety of synthetic options for their incorporation in active compounds and polymers. Several research groups screened the available catechol containing compounds and elaborated coupling strategies depending on the additional functional groups present in the structure. Most examples focused on the use of natural compounds which share common biosynthetic routes with dopamine, as L-DOPA or caffeic acid and their derivatives. Moreover, catechol containing compounds can be directly linked to the desired molecule or be subjected to prior activation as in the case of hydrazides. Fig. 2 offers an overview of the catechol molecules and the respective linking chemistry.

### Levodopa

Levodopa (L-DOPA), a naturally occurring amino acid, was individuated as the adhesive unit of mussels foot proteins (Mfps).<sup>6,11</sup> It should not surprise that the synthetic exploration of adhesive catechol materials started with the preparation of L-DOPA containing peptides. Nonetheless, as we will further detail in this text, catechol compounds reactivity poses limitations, and often requires the use of protecting groups to prevent side reactions. This was soon discovered in attempting the inclusion of L-DOPA in conventional peptide synthesis. A number of approaches have been successfully applied for the protection of both catechol and amino groups. For the latter, Fmoc or Boc protecting groups were the most common. The protection of catechol was instead tackled in a variety of ways. An early example from Yu and Deming described the use of O,O'-dicarbobenzoxy-L-DOPA NCA for the preparation of L-DOPA-L-lysine adhesive peptides.<sup>18</sup> Later, Messersmith and coworkers reported the preparation of protected L-DOPA to be employed in Fmoc solid-phase peptide synthesis.<sup>19</sup> This entailed a five steps synthetic procedure to obtain Fmoc-DOPA (Ceof)-OH (Scheme 1). This could then deliver the free amine or free catechol selectively through treatment with either piperidine or TMSBr.

The same group later reported also the preparation of Fmoc-dopa(acetonide)-OH.<sup>20</sup> This required the protection of L-DOPA as phthalimide methyl ester (Scheme 2). The catechol

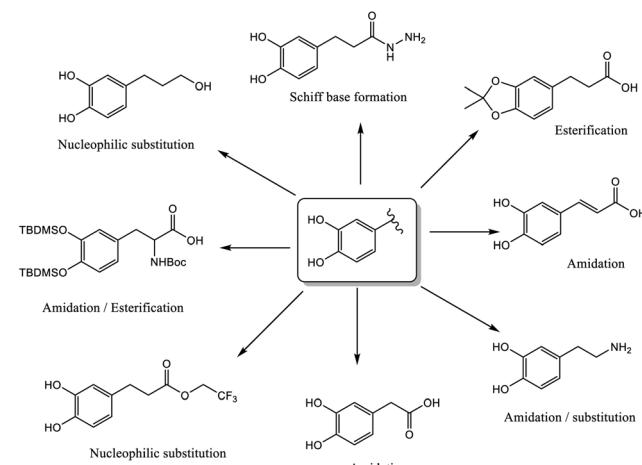
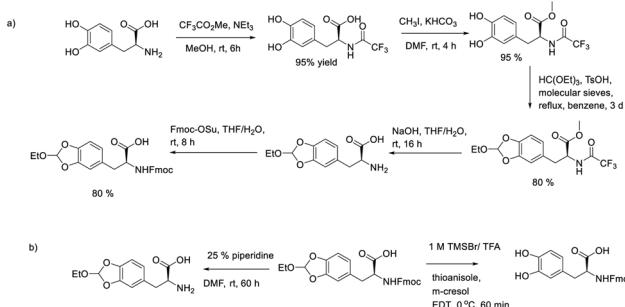
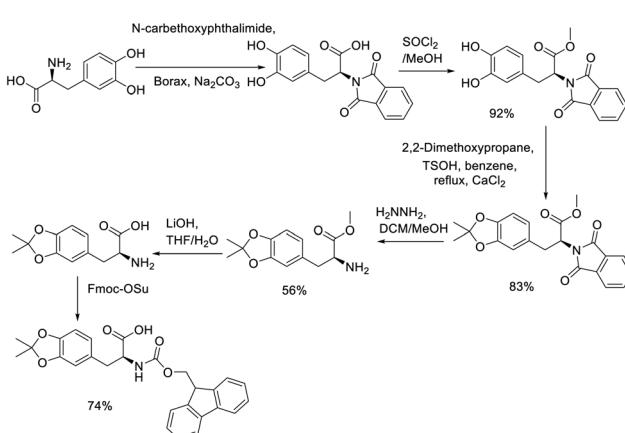


Fig. 2 Various coupling strategies for catechol incorporation.





**Scheme 1** a) Synthetic procedure of Fmoc-DOPA(Ceof)-OH and (b) deprotection procedure of Fmoc and cyclic ethyl orthoformate (Ceof).



**Scheme 2** Synthesis of Emoc-dopa(acetonide)-OH.

was protected by reaction with 2,2-dimethoxypropane (DMP) in anhydrous benzene and with TsOH as a catalyst. As in this reaction an equilibrium establishes, the flask was equipped with a Soxhlet extractor filled with  $\text{CaCl}_2$  to trap water and methanol produced, favoring conversion to the acetonide. Upon formation of the catechol acetonide, the aminoacidic residue was restored by sequential treatment with hydrazine and  $\text{LiOH}$ .

In a paper from Statz *et al.* Fmoc-DOPA(acetonide) was employed in the preparation of an anchoring peptide, composed of alternating L-DOPA and lysine. This was coupled with a peptoid composed of repeating *N*-methoxyethyl glycine units (Fig. 3).<sup>21</sup> The obtained peptidomimetic polymer showed good adherence and promising antifouling activity. Later, this approach was further explored by K. H. A. Lau and coworkers in designing a similar polymer consisting of *N*-methylglycine (sarcosine).<sup>22</sup> Polysarcosine containing DOPA-Lys pentapeptide (PSAR brush) was grafted on TiO<sub>2</sub> to achieve highly hydrophilic surfaces (water contact angle 20–30°) with antifouling property. PSAR brushes were shown to resist fibroblast cell attachment over a 7 weeks period, and also resist the attachment of some clinically relevant bacterial strains.

Kuang and Messersmith exploited the same chemistry for the preparation of a short adhesive peptide (DOPA-Lysine- $\text{Glycine}_2$ ).

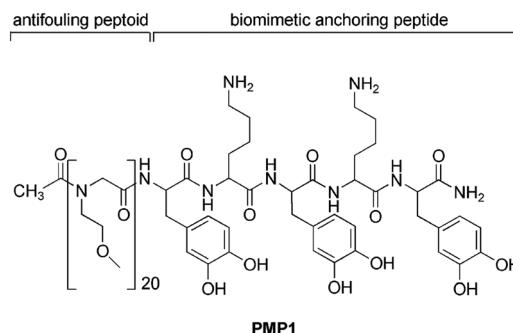
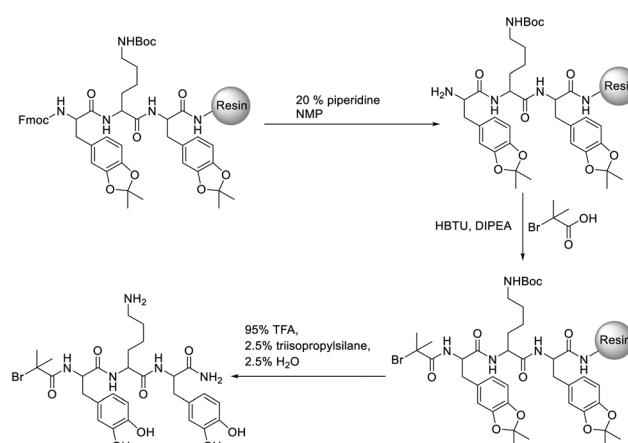


**Fig. 3** Antifouling peptidomimetic polymer (PMP). Reproduced with permission from ref. 21. Copyright 2005 American Chemical Society.

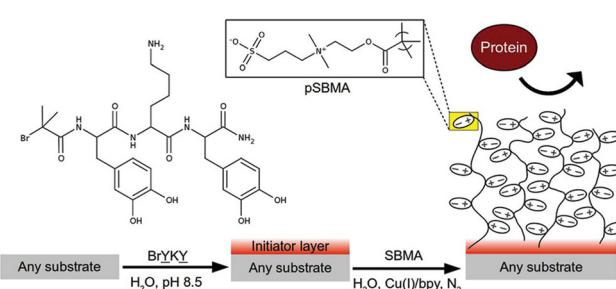
DOPA) modified with 2-bromo-2-methylpropionic acid to allow further functionalization with sulfobetaine methacrylate (SBMA) *via* ATRP (Scheme 3 and Fig. 4).<sup>23</sup>

TiO<sub>2</sub> coated silicon wafers were functionalized through dip coating in a solution of the synthetized initiator with bicine buffer at pH 8.5, and provided a reactive surface for ATRP.

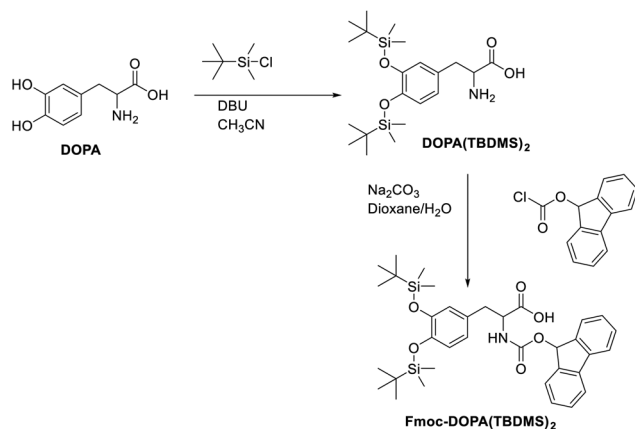
Sever and Wilker proposed the preparation of Fmoc-L-DOPA-TBDMS, which is also compatible with peptide synthesis (Scheme 4).<sup>24</sup> L-DOPA was first reacted with *tert*-butyldimethylsilyl



**Scheme 3** Synthesis of 2-bromo-2-methylpropionic acid derivative of DOPA-Lysine-DOPA



**Fig. 4** Surface modification with SBMA via ATRP. Reproduced with permission from ref. 23. Copyright 2012 American Chemical Society.

Scheme 4 Synthesis of Fmoc-DOPA(TBDMS)<sub>2</sub>.

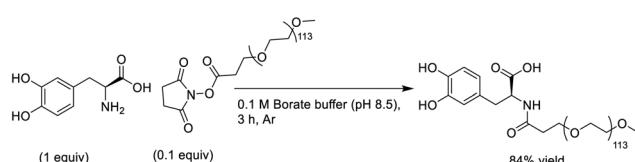
silyl chloride to protect the catechol ring. This is followed by reaction with Fmoc-Cl.

In the same paper the procedure was applied to the synthesis of a peptide residue from the adhesive protein Mefp-3 of the common blue mussel *Mytilus edulis*. Interesting is also the use of ammonium fluoride salts for catechol deprotection in combination with TFA.

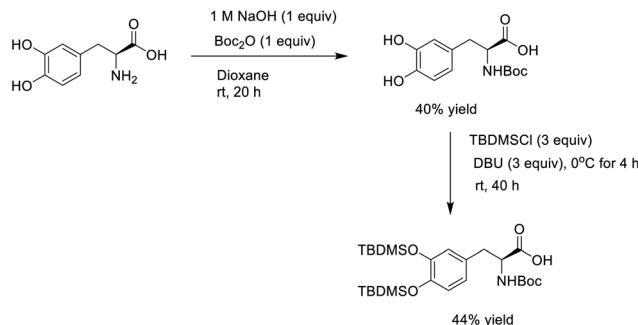
The scope of application for L-DOPA anchor strategies is not limited to peptides. The carboxylic acid group in levodopa provides a site for modification, perhaps through an amide bond with an amino group in the active molecule. At the same time, the coupling products still contain a primary amine which improves water solubility and also acts as a nucleophile for Michael addition during polymerization, to form the dopamine type intermediates described in poly-catecholamine films.<sup>25</sup> For these reasons, levodopa appears as an ideal candidate for direct modification through covalent attachment of target molecules.

Dalsin *et al.* investigated the surface adsorption and protein resistance behavior of polyethylene glycol-DOPA conjugate (mPEG-DOPA) on a titanium oxide film for the development of non-fouling surfaces.<sup>26,27</sup> For the synthesis of mPEG-DOPA, L-DOPA was stirred in 0.1 M borate buffer (pH 8.5) under inert atmosphere, to prevent oxidation of the catechol group and side reactions. This was followed by the addition of succinimidylpropionate activated PEG (mPEG-SPA) (Scheme 5). Borate-catechol interactions will be described in more detail in the next section.

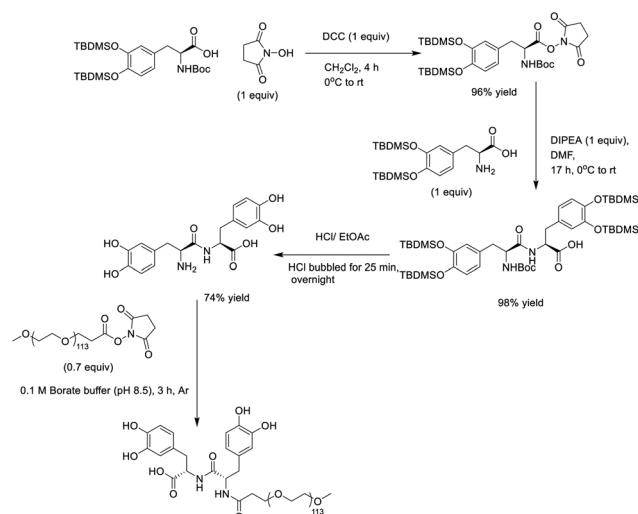
Analogues comprising of L-DOPA dimer and trimer were also prepared through sequential amide bond synthesis with



Scheme 5 Synthesis of mPEG-DOPA.



Scheme 6 Reaction scheme for the protection of L-DOPA.

Scheme 7 Reaction scheme of the synthesis of mPEG-(DOPA)<sub>2</sub>.

protected L-DOPA *N*-hydroxysuccinimide ester (Schemes 6 and 7). The surface absorption profile showed strong dependence of the coating efficiency, in terms of thickness, on the number of catechol groups (Fig. 5).

Pegylation has also been reported also *via* functionalization of the L-DOPA carboxylic acid moiety. Ki *et al.* also followed a similar procedure involving protection, coupling and deprotection to modify levodopa with hexaethylene glycol (EG6), for the development of an antibacterial thin film on titanium oxide (Ti/TiO<sub>2</sub>) surfaces.<sup>28</sup> Mono-TBDMS protected hexaethylene glycol (EG6-TBDMS) was reacted with protected DOPA in dichloromethane, using DCC as coupling reagent and DMAP as base (Scheme 8).

The ethylene glycol derivative of DOPA (OEG-DOPA) was polymerized *via* oxidative polymerization and complexation with iron ions (Fe<sup>3+</sup>). The oxidative polymerization of OEG-DOPA was carried out using NaIO<sub>4</sub> as oxidant in the presence of FeCl<sub>3</sub>. Complexation of Fe<sup>3+</sup> ions by the catechol of OEG-DOPA allowed the crosslinking between the glycol chains. This is followed by polymerization *via* oxidation-induced covalent coupling (Fig. 6). Reaction conditions reflected in

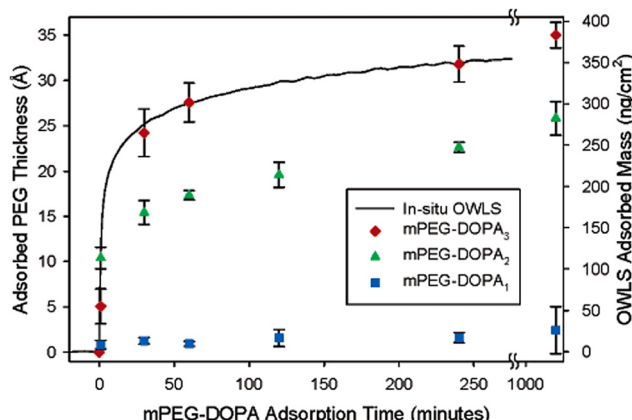
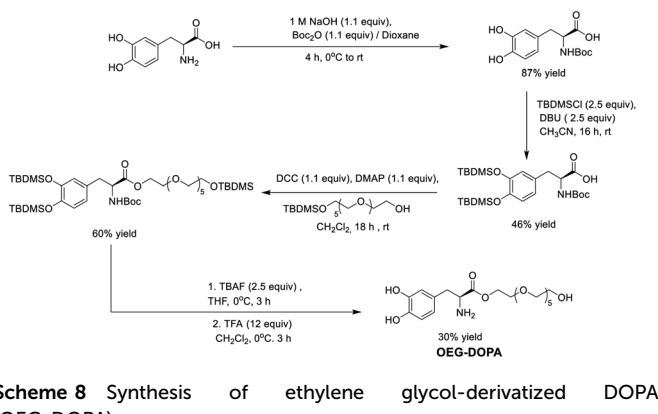


Fig. 5 Time-dependent adsorption of mPEG-DOPA onto  $\text{TiO}_2$ . Reproduced with permission from ref. 27. Copyright 2005 American Chemical Society.



Scheme 8 Synthesis of ethylene glycol-derivatized DOPA (OEG-DOPA).

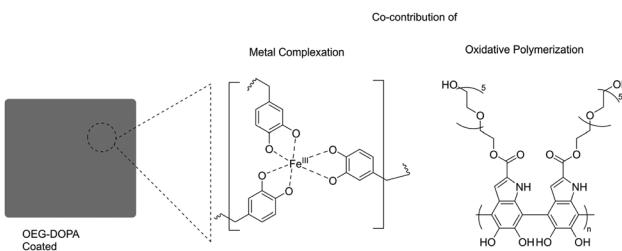


Fig. 6 Antibacterial film formation of OEG-DOPA via complexation and oxidative polymerization.

both thickness and contact angle values of the resulting coatings (Fig. 7).

Wohlek *et al.* developed nitroxide-containing polymer films on hydroxyapatite and titanium surfaces for biofilm inhibition using TEMPO as the active component.<sup>29</sup> As nitric oxide (NO) is a key molecule in the regulation of biofilm development, nitroxide-functionalized surfaces mimicked the properties of NO and disrupted biofilm formation on *Pseudomonas aeruginosa*. To synthesize the TEMPO conjugate of levodopa

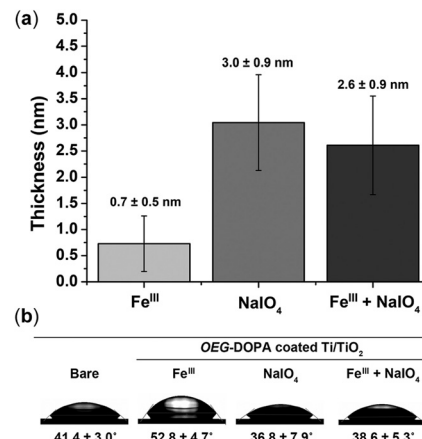
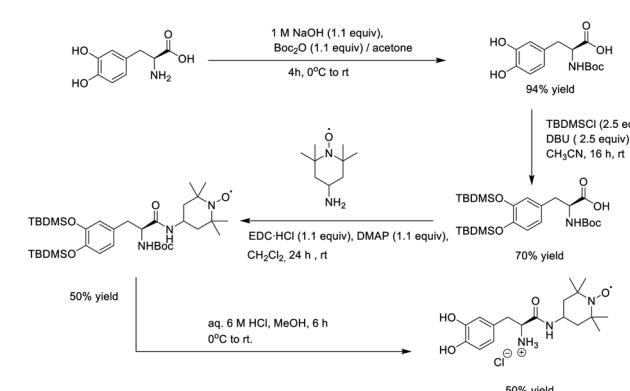


Fig. 7 (a) Film thickness and (b) static water contact angles of OEG-DOPA-coated substrates prepared at different conditions. Reproduced with permission from ref. 28. Copyright 2019 American Chemical Society.



Scheme 9 Synthesis of TEMPO-DOPA conjugate.

(Scheme 9), the hydroxyl and amine groups of L-DOPA were protected with *tert*-butyldimethylsilyl chloride (TBDMSCl) and Boc-anhydride (Boc<sub>2</sub>O), respectively. The protected L-DOPA was then coupled with 4-amino-TEMPO. Finally, deprotection under acidic conditions resulted in the hydroxylamine hydrochloride salt.

Hydroxyapatite samples, employed in the antibiofilm activity tests, were functionalized with DOPA-TEMPO conjugate by dip coating in Tris-HCl buffer at pH 9.25. One other interesting application was the use of UV photolithography to spatially controlled surface immobilization of nitroxide-containing polymers on titanium substrates. This was performed optimizing a coating solution that would not spontaneously set on polymerization in dark conditions. Then, upon UV irradiation ( $\lambda_{\text{max}} = 313$  nm) reactive *o*-quinone intermediates were formed, kickstarting polymerization on the target surface. This allowed for sub-millimeter spatial resolution of the coated area (Fig. 8).

The two-step preparation of zwitterionic surfaces *via* ATRP with reactive adhesive L-DOPA peptide was mentioned earlier



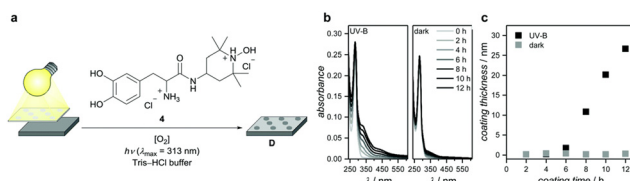


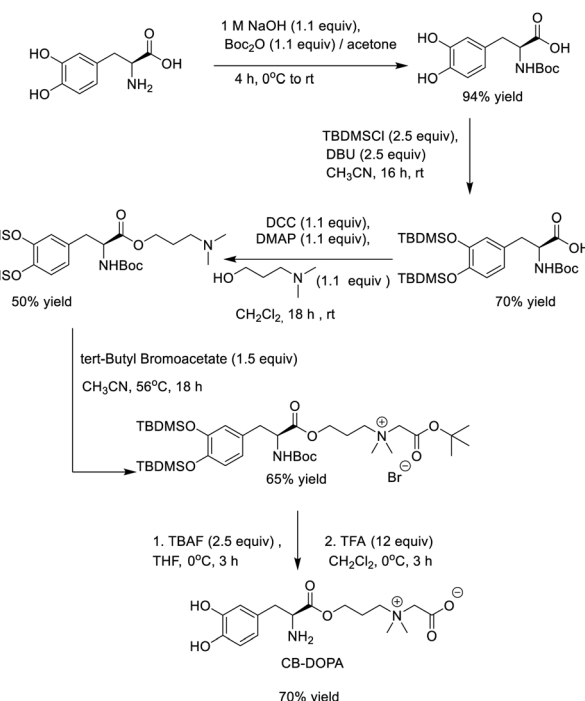
**Fig. 8** Light-induced polymer film formation on surfaces generating spatially confined antibiofilm domains. (a) Synthetic route for the photopolymerization onto titanium substrates. (b) UV-vis spectroscopic monitoring of catechol oxidation and catecholamine polymerization. (c) Coating thickness of polymer films deposited on silicon substrates under UV irradiation. Reproduced with permission from ref. 29. Copyright 2019 Royal Society of Chemistry.

in this chapter. Yeon *et al.* proposed a simplified route to sulfobetaine antifouling coatings.<sup>30,31</sup> The new approach sees the reaction between the *N,N*-dimethylaminopropoxy levodopa conjugate and 1,3-propanesultone, followed by further deprotection, to obtain a zwitterionic sulfobetaine-levodopa derivative (ZW-DOPA) (Scheme 10).

This would undergo oxidative polymerization by addition of NaIO<sub>4</sub> in a 2 : 1 molar ratio, and form a coating on Ti/TiO<sub>2</sub> substrates.

Similarly Han *et al.* prepared antifouling surfaces by mean of a carboxybetaine levodopa conjugate.<sup>30</sup> The synthesis involved the esterification of protected levodopa and (3,4-dimethylamino)propan-1-ol, using DCC and DMAP as coupling reagents in dichloromethane, to yield the *N,N*-dimethylaminopropoxy levodopa conjugate. The resulting compound was treated with *tert*-butyl bromoacetate and deprotected with TBAF and TFA, thereby forming a carboxybetaine conjugate of levodopa (Scheme 11). A uniform coating on gold surface, with a thickness of 53 nm, was obtained employing sodium periodate as oxidant.

Ukita and colleagues investigated various poly(carboxybetaine) (pCB) coating methods for artificial lung surfaces and

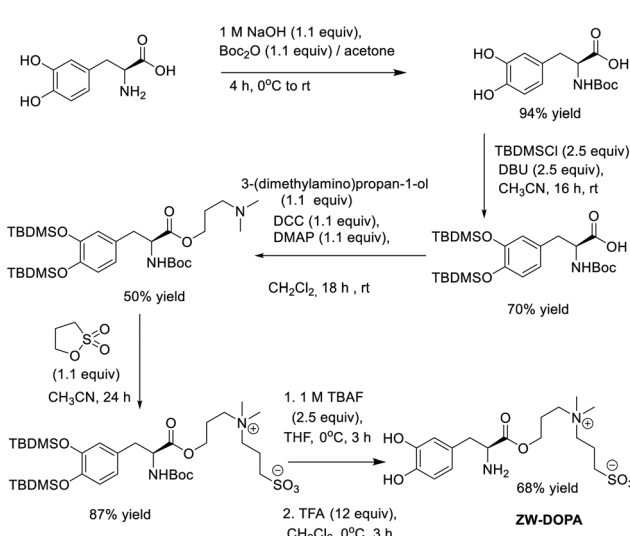


**Scheme 11** Synthesis of carboxybetaine DOPA zwitter ion.

evaluated their biocompatibility in sheep and rabbit models.<sup>32</sup> Their study demonstrated the superiority of the DOPA-poly(carboxybetaine) (DOPA-pCB) conjugate for surface fabrication compared to two other approaches: surface-initiated polymerization of pCB (“graft-from”) and co-deposition of pCB with a hydrophobic copolymer.

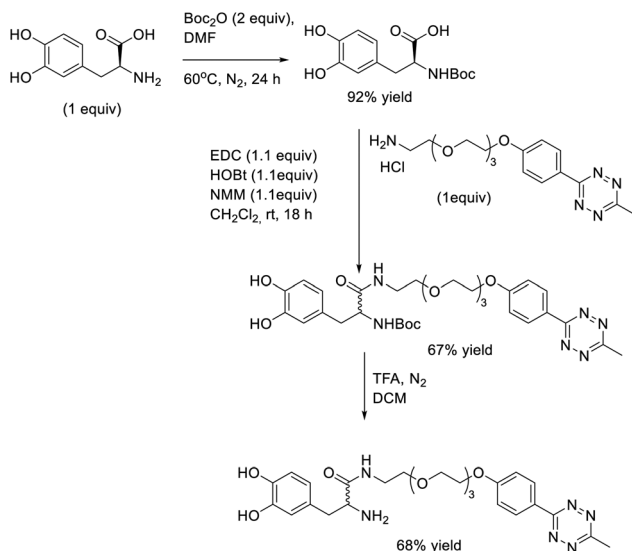
Among the three methods, the DOPA-pCB coating exhibited the lowest failure rate and the most consistent performance. Although the graft-from method enables high grafting density through covalent attachment of initiator molecules and subsequent polymerization of CB monomers, it was only marginally more effective than the uncoated control and remains costly and complex for large-scale application. The co-deposition approach, while widely adopted in industry, showed substrate-dependent efficiency and resulted in a faster increase in blood flow resistance compared to the uncoated control. This study represents a clear example how the direct modification approach can improve surface modification in terms of procedural simplicity and coating performances.

Hast *et al.* reported the synthesis of DOPA-Tetrazine (DOPA-Tet) complex to graft molecules of interest to surfaces via tetrazine/trans-cyclooctene (TCO) cycloaddition.<sup>33</sup> The amine group of DOPA was protected with Boc<sub>2</sub>O in DMF, and (3-phenyl-6-methyl-1,2,4,5-tetrazine)-PEG4-amine (Tet-PEG4-NH<sub>2</sub>) was synthesized via EDC/HOBt coupling. Use of *N*-methylmorpholine (NMM) facilitated the coupling reaction. However, this resulted in racemization of L-DOPA (Scheme 12). This aspect is often overlooked as it is not expected to influence the adhesive role of DOPA, and is therefore rarely mentioned in reports.



**Scheme 10** Synthesis of sulfobetaine DOPA zwitter ion.





Scheme 12 Synthesis of DOPA-Tetrazine (DOPA-Tet) complex.

An interesting approach was chosen for the immobilization of the DOPA-Tet conjugate. Polymerization on the substrate surface (polypropylene and polyethylene terephthalate) was enzymatically performed employing tyrosinase enzyme. Molecules of interest as peptides, vancomycin, and enzymes (HRP, Gox, ALP) were modified with *trans*-cyclooctene (TCO) to allow grafting on the Tet-DOPA coating *via* Tet-TCO ligation (Fig. 9). Although the surface modification process consists of a coating and a grafting step they are subsequently performed in a one-pot fashion.

### Dopamine and other catecholamines

**Dopamine.** Since its discovery, the landscape of catechol coatings has seen the predominant use of dopamine as building block. Nonetheless, this mainly regarded the preparation of polydopamine coatings and particles, without prior modification of the catechol source. Therefore dopamine based func-

tional coating usually rely on multistep processes or co-deposition with the active molecule. The preparation of dopamine conjugates with small molecules is an appealing approach for surface functionalization in a variety of applications as it allows for better surface coverage and homogeneity.<sup>34</sup> In here, we will focus on selected example where dopamine is exploited to impart adhesive properties to molecules of interest and allow surface modification with a variety of functional groups.

Looking at the chemical structure of dopamine, the primary amino group offers accessible synthetic pathways for its modification. Primary amines can participate in amide bond formation and can also act as nucleophiles in substitution reactions. Nonetheless, when it comes to dopamine, specific precautions need to be taken, as the aforementioned reactions usually take place in basic conditions which would cause polymerization to polydopamine. An early example of dopamine direct modification was reported by Messersmith's group (Scheme 13a) where they approached polymer adhesion on the substrate through surface initiate atom transfer polymerization (SI-ATRP; graft from vs. graft to approach).<sup>35,36</sup> To this end, a 2-bromopropionyl amide derivative of dopamine was prepared. Upon adhesion on the sample surface it served as radical initiator for the polymerization of methyl acrylate *via* SI-ATRP.<sup>35</sup> Although the overall protocol consists of a multi-step coating procedure, it entailed the preparation of a reactive and adhesive surface modifier which is within the scope of this review. Of particular interest are the reaction conditions employed for the functionalization of dopamine with 2-bromopropionyl bromide (Scheme 13a). Both the addition of borax and the use of inert atmosphere are crucial to avoid the polymerization of dopamine while working at high pH values. On the one hand oxygen-free conditions prevent oxidation of catechol to quinone and consequent polymerization as well as side reactions with nucleophiles. On the other hand, the instauration of a catechol boron complex hampers catechol grafting and film formation. Moreover, catechol borate esters are easily hydrolyzed in acidic condition during the workup. This synthetic approach resulted in a moderate yield of 33%. The same group reported the use of sodium borate, with the same reaction conditions, in the reaction of dopamine and methacrylate anhydride to form dopamine methacrylamide (DMA) with a yield of 78% (Scheme 13b).<sup>37</sup> This was then

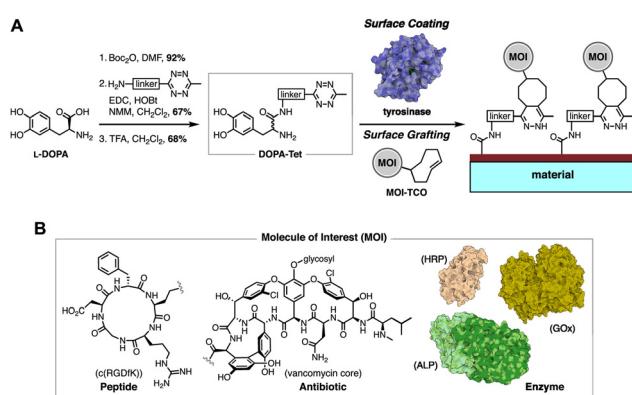
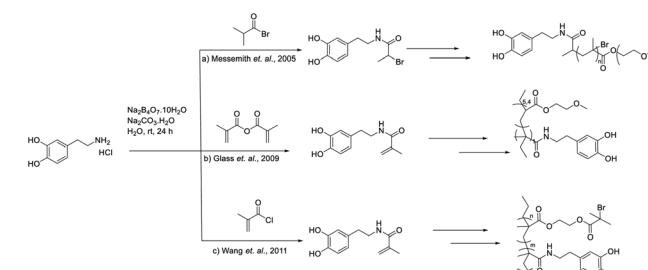


Fig. 9 Overview of the bioorthogonal material surface functionalization *via* Tet-TCO ligation of molecules of interest (MOIs) through L-DOPA grafting. Reproduced with permission from ref. 33. Copyright 2019 American Chemical Society.



Scheme 13 Use of borax for modification of dopamine.



employed in the preparation of an adhesive catechol rich polymer through polymerization with 2-methoxyethyl acrylate.

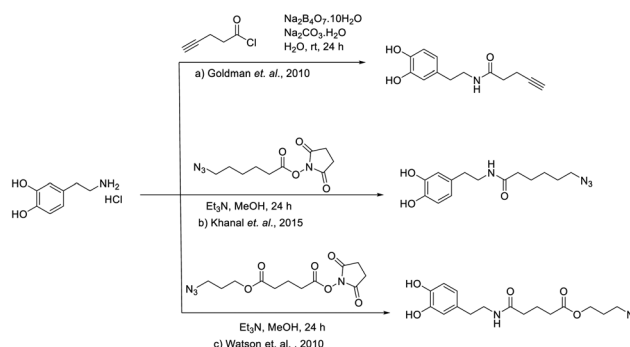
In a later paper from Wang *et al.* these two strategies were joined together towards the production of an acrylate based polymer suitable for SI-ATRP.<sup>38</sup> Two methyl acrylate copolymers carrying a catechol and an  $\alpha$ -bromo ester respectively, were let react to form an adhesive polymer which could be further modified *via* SI-ATRP (Scheme 13c).

The same reaction conditions were also successfully employed by Kohri *et al.* in the coupling of dopamine with acryloyl chloride.<sup>39</sup> Prior to further modification through Raft polymerization, the intermediate was reacted with 2,2-dimethoxypropane for the protection of catechol, as acetonide. The latter being sensitive to visible light and acids, allowed for a timed activation of the adhesive properties. These could then be activated *via* acid or photo induced acetonide cleavage.

The influence of boric and boronic acid on dopamine polymerization and adhesion has been further investigated more recently. As reported by Schneider *et al.* the formation of a complex with boric acid causes a shift of the oxidation potential of around 0.4–0.6 V resulting in no film formation in an oxygenated solution at pH = 8.5 (Fig. 10).<sup>40</sup>

Nonetheless, the oxidation during CV was irreversible and after several scans a film formed on the electrode. Similar inhibition was obtained with boronic acid in line with the results obtained by Belitsky *et al.* in the case of L-DOPA.<sup>41</sup> Interestingly, a recent paper described the formation of ultrathin films at the air liquid interface when dissolving DA and BA at a ratio between 1:3 and 1:6 where 5,6-dihydroxyindole (DHI) and 5,6-indolequinone (IDQ) units were held together *via* hydrogen bonding and  $\pi$ – $\pi$  interactions into a physical assembly.<sup>42</sup>

The synthesis of dopamine analogues is a versatile tool for the preparation of surfaces decorated with reactive functional groups. Goldmann *et al.* and Watson *et al.* developed specular approaches towards “clickable” surfaces, by employing dopamine based anchors bearing respectively an alkyne or an azide as functional group. In both cases an amide bond was formed



**Scheme 14** Functionalization of dopamine with an alkyne/azide group.

with the coupling partner but following different pathways (Scheme 14).<sup>43,44</sup>

Goldman *et al.* employed the reaction conditions discussed above for the preparation of an alkyne derivative of dopamine using pentynoic acid chloride as coupling partner (Scheme 14a).<sup>43</sup> The authors mention that a brownish liquid was obtained after workup suggesting a certain degree of catechol oxidation. Nonetheless, the product could be isolated as a clear liquid through column chromatography and in a 41% yield. Grafting onto iron oxide nanoparticles was performed in hexane and applying ultrasounds for 45 min.

In the case of azide bearing catechol ligand an amide bond was formed between dopamine and azidopropyl succinate *N*-hydroxysuccinimide ester (Scheme 14c).<sup>44</sup> The reaction was carried out in methanol, through dropwise addition of the ester to a solution of dopamine and Et<sub>3</sub>N, and gave the desired product at 80% yield and as a light brown solid. It is worth noticing that the reaction in an organic solvent worked smoothly, even in the absence of borate or boronic acid. The adhesion on titanium surface, activated by treatment with piranha solution, was performed *via* dip coating in a 1 mM methanol solution of the catechol azide anchor, at room temperature and overnight. In both cases further functionalization was easily carried out *via* CuAAC reaction (Scheme 15).

In 2021, Putnam *et al.* prepared a dopamine-methyl methacrylate monomer by reaction with methacrylic anhydride and forming a stable amide bond.<sup>45</sup> Adhesive polymers with varying catechol contents were prepared employing different

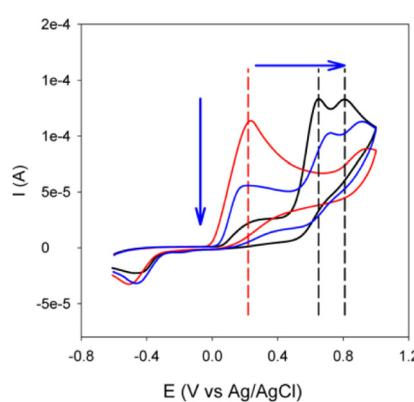
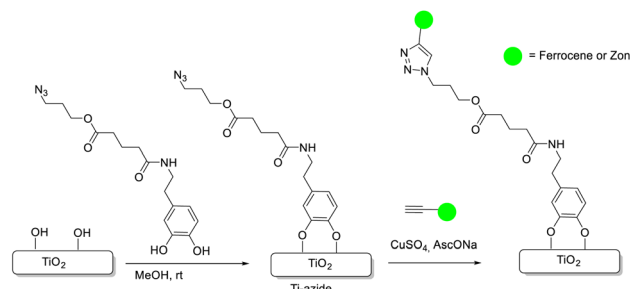


**Fig. 10** CV curves of dopamine at 3.5 mM in Tris buffer (red line), in Tris buffer containing 43.0 mM boric acid (blue line), and in Tris buffer containing 430 mM boric acid (black line). Reproduced with permission from ref. 40. Copyright 2017 American Chemical Society.



**Scheme 15** Functionalization of surface with azide catechol via CuAAC reaction.

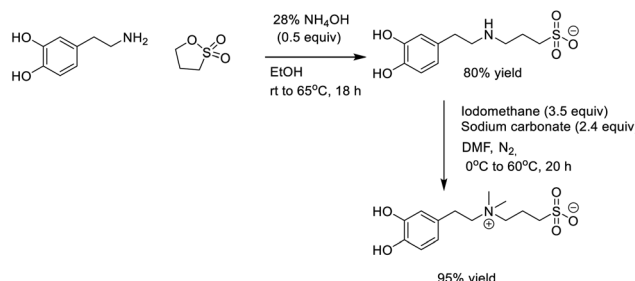


ratios of modified methyl methacrylate (MMA) in the reaction with oligo(ethylene glycol) (OEG). Adhesion strength was maximized at ~10 mol% catechol for high-energy aluminum and ~41 mol% for low-energy Teflon. The catechol content also influenced wettability, failure modes, and mechanical behavior, highlighting the need to balance adhesive and cohesive properties.

Amide bond synthesis was employed also by Wei *et al.* in the preparation of an adhesive hyperbranched polyglycol (hPG).<sup>46</sup> First, carboxylic acid moieties were introduced in the hPG structure through reaction with succinyl anhydride. Amide synthesis with dopamine was carried out with conventional peptide coupling conditions (*i.e.* BOP, HOBT, DIPEA in DMF) (Scheme 16).

Despite the accessible synthetic pathways for dopamine modification, the effect on the coating ability is not easily predicted, leading to non-trivial optimization of the coating conditions. This probably concur to the limited number of publications on the incorporation of dopamine, mainly focused on the functionalization of nanoparticles, as common conditions for the preparation of polydopamine coatings would likely fail. An instructive example was published by Huang *et al.* where they developed an adhesive zwitterionic sulfobetaine analogue of dopamine (SB-DA) and described its adhesive properties in the surface modification of TiO<sub>2</sub>.<sup>47</sup> SB-DA was prepared, as previously reported, by reacting with 1,3-propanesultone, acting as an electrophile, with subsequent treatment with iodomethane to afford the desired zwitterion (Scheme 17). The newly obtained dopamine analogue is characterized by a bulky and positively charged ammonium group and is not able to undergo the same route toward the formation of dopachrome intermediates described in the preparation of polydopamine coatings. The effect on the redox properties of the catechol moiety was investigated using cyclic voltammetry.

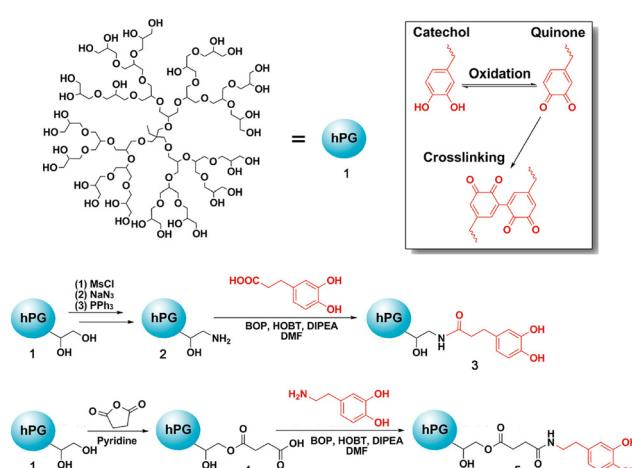
This was performed on a 5 mM solution of both dopamine (DA) and SB-DA at pH 3 and pH 8. At pH 8, for both DA and



**Scheme 17** Synthesis of a sulfonate zwitter ionic derivative of dopamine.

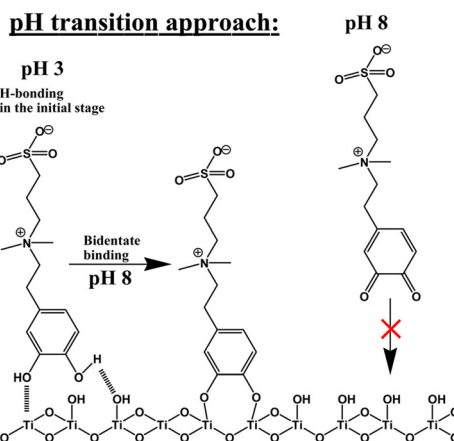
SB-DA, the current densities decreases with the number of scans and the reverse peaks in the potential axis were hardly extrapolated. This was due to polydopamine formation for DA and, in the case of SB-DA, to the irreversible oxidation to SB-1,2-benzoquinone. However, at pH 3 the redox properties were reversible and current densities did not drop significantly after multiple scans. This reflected also in surface modification experiments. Whilst dopamine formed adhesive polydopamine films in alkaline conditions, samples dipped in a SB-DA solution at pH 8 showed low coverage. Interestingly, the coverage was even lower than samples prepared at pH 3 as is evident from the more significant change in contact angle. This can be explained looking at the reactivity of catechol. As indicated by the CV experiment, at pH 8 SB-DA irreversibly oxidizes to quinone form, which is more reactive toward nucleophiles *via* Michael-type or Schiff-base reactions. At low pH instead, catechol oxidation is inhibited. This allows adhesion by hydrogen bonding, or chelation of metals surfaces. The authors described a pH transition approach where the substrates were dipped to SB-DA solution of pH 3 and subsequently transferred to a pH 8 buffer, referred as SB-DA(3-8). At low pH catecholic OH groups undergo hydrogen bonding on the hydroxylated TiO<sub>2</sub> surface. Then, as the pH increases, they form bidentate metal-oxide bonds by the replacing the hydroxyl groups on the titanium surface (Scheme 18) as suggested by XPS analysis of the O 1s signal corresponding to C-O-H/C-O-Ti/Ti-OH bonds. Differences in surface coverage were further supported by assessing the anti-fouling properties which peaked for SB-DA(3-8) plates. Reduction rates in bacterial adsorption, compared with the bare TiO<sub>2</sub> surface, reached 96.9% and 97.4% for *P. aeruginosa* and *S. epidermidis* respectively. Later the same group, applied this strategy for the preparation of a zwitterionic polymer coating on nitinol.<sup>48</sup> In this case short polymer chains were produced from a mixture of dopamine sulfobetaine methyl acrylate upon UV irradiation *via* dopamine-initiated photo-polymerization (Fig. 11). The polymer particles were then let adhere on the substrate surface at pH 3 followed by pH transition by immersion into a pH 8 Tris-HCl buffer to obtain a stable coating.

In 2016, Xu *et al.* synthesized a catechol containing PEG functionalized with sulfobetaine (SBCaPEG).<sup>49</sup> First poly(ethylene glycol) (CaPEG) was prepared *via* epoxide–amine polymer-



**Scheme 16** Synthesis of catechol functionalized hyperbranched polyglycerols (hPGs). Reproduced with permission from ref. 46. Copyright 2014 American Chemical Society.





**Scheme 18** Binding mechanism of the SB-DA molecules with the pH transition approach and under oxidation at pH 8. Reproduced with permission from ref. 47. Copyright 2014 American Chemical Society.

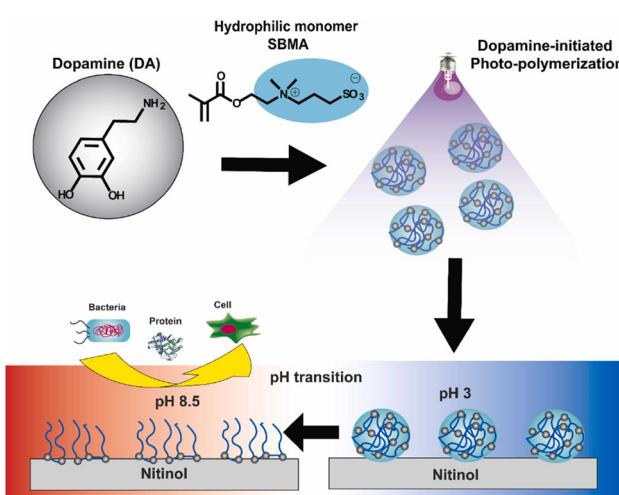


**Fig. 11** pSBMA/DA synthesized via dopamine-initiated photo-polymerization method and deposition on nitinol through pH-induced aggregation formation. Reproduced with permission from ref. 48. Copyright 2022 Elsevier.

ization of PEG diglycidyl ether with dopamine. Subsequent alkylsulfonation with 1,3-propanesultone converted the tertiary amine groups into sulfobetaine structures. The functionalized polymer readily anchored onto stainless steel, titanium, and silicon surfaces under mild conditions. The coated surfaces showed reduced protein adsorption and inhibited bacterial (*Pseudomonas* sp., *E. coli*) and microalgal (*Amphora coffeaeformis*) adhesion, decreasing viable cell numbers to approximately 8% of those on uncoated surfaces.

**Anachelin analogues.** Anachelin is a natural compound secreted by cyanobacteria, and is characterized by a 3,4-dihydroxyquinolinium unit (Anacat). The latter has the ability to coordinate iron ions with high affinity even at low concentrations. In environments, as marine systems, characterized by

low iron availability, anachelin acts as a siderophore improving iron intake which would otherwise limit bacterial growth.<sup>50</sup> The preparation of the anacat unit was described by Gademann, and was soon applied by his group for the preparation of adhesive polymers.<sup>51-53</sup>

The anacat structure offers some advantages compared to dopamine (Fig. 12). The permanent positive charge, of the quaternary amine, increases the stability toward oxidation while lowering the  $pK_a$  of the catecholic -OH groups. At the same it was suggested that better coating performance could be obtained on negatively charged surfaces by electrostatic interactions. In the first report from Zürcher *et al.* anacat PEG-conjugate was prepared and compared with dopamine and L-DOPA analogues (Fig. 13).<sup>54</sup> In all cases the catechol substrate was linked with the PEG chain through amide bond by reacting with *N*-hydroxysuccinimide ester-poly(ethylene glycol) in the presence of *N*-methylmorpholine, providing the desired products in moderate to good yields. Anacat-PEG polymer outperformed both dopamine and L-DOPA analogues in terms of layers thickness when deposited on  $\text{TiO}_2$  surface. Electrostatic interaction between the anacat unit and the negative charges of the hydroxylated  $\text{TiO}_2$  surface could explain the higher bonding strength. Contrarily, the L-DOPA analogue carrying a negatively charged carboxylate, failed adhering to the surface.<sup>55</sup> The improved surface coverage was also proven *via* serum absorbance experiments, to evaluate antifouling properties. Similar protein resistant behavior was also reported when using a modified dopamine analogue carrying a trimethyl ammonium-methylene group.<sup>55</sup> Finally, anacat-PEG showed higher stability in aerobic conditions as compared to the dopamine derived polymer.

A later publication from Watch *et al.* incorporated vancomycin at the end of the PEG chain for the preparation of an antimicrobial surface (Fig. 14).<sup>56</sup> An aminated analogue of anacat-PEG was prepared using the bifunctional Fmoc-NH-PEG-succinimidyl ester under the same reaction conditions described above. Fmoc cleavage followed by amide bond formation with anacat gave the desired product. Surface modification was carried *via* simple dip coating in MOPS (3-(*N*-morpholino)propanesulfonic acid) buffer. The coated substrate showed good

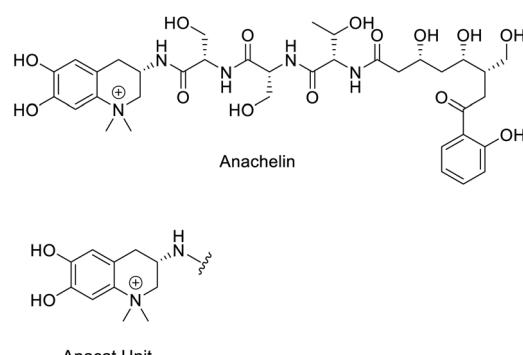


**Fig. 12** Chemical structure of anachelin and the anacat unit.



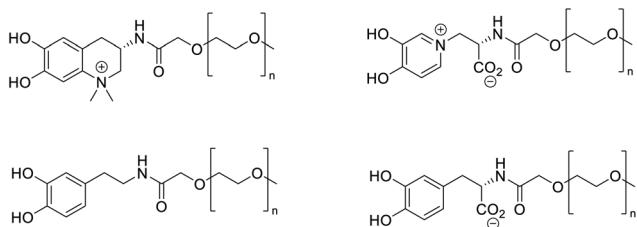


**Fig. 13** Chemical structure of PEG-conjugate of catechol derivatives.

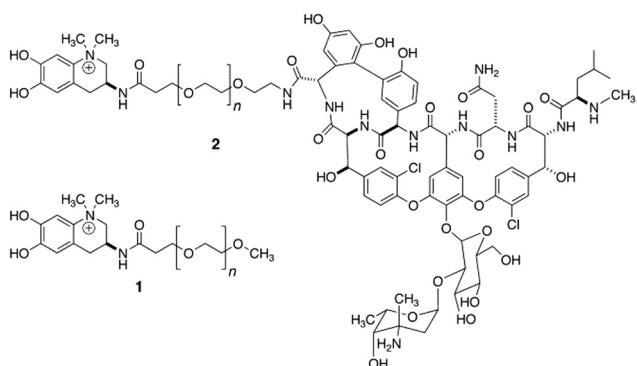


**Fig. 14** Chemical structure of vancomycin and PEG modified anatac. Reproduced with permission from ref. 56. Copyright 2008 John Wiley and Sons.

antimicrobial activity together with low adherence of dead cells, thanks to the PEG chain linker.

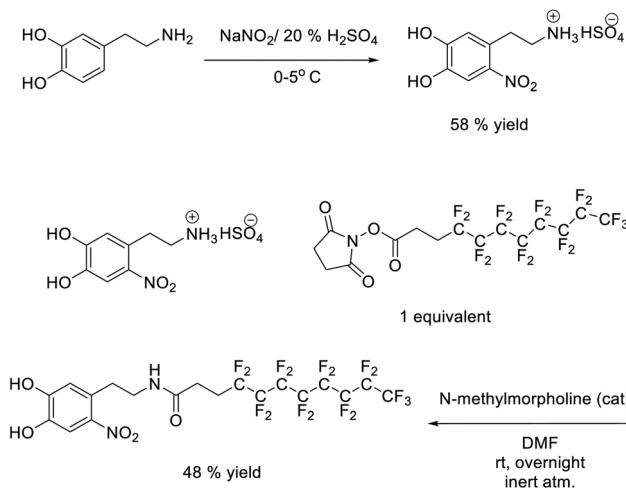
**Nitrodopamine.** The studies on anachelin showed how the permanent positive charge of the quaternary amine could enhance the iron ions binding capability of catechol. Further research described the effect of other electron withdrawing groups as higher acidity catecholic hydroxyl groups and stronger affinity for metal oxides.<sup>57,58</sup> Among others, the nitro group effectively lowers the dissociation constants of the catechol hydroxyl groups ( $pK_a = 6.6$  and 11 for 4-nitrocatechol compared to  $pK_a = 9.2$  and 14 for catechol).<sup>59</sup> This is confirmed by the higher interfacial binding strength of 6-nitrodopamine.<sup>60</sup> Moreover, Cencer *et al.* reported how *N*-PEG-nitrodopamine adhesive properties remained unchanged in a wide pH range (5.7–8), allowing for higher loading in slightly acidic conditions as compared to the dopamine analogue, which would perform better only within a narrow pH range.<sup>61</sup> In addition, the substitution with a nitro group causes an increase in redox potential as the catechol ring becomes less electron-rich. This would in turn, increase the stability towards oxidation at high pH values. Finally, substitution on the phenyl ring results in lower tendency to form polymers as compared to dopamine, and mainly crosslink through dimerization<sup>61,62</sup>

Amstad *et al.* reported the functionalization of metal nanoparticles with PEG chains linked to a variety of catechol anchors, including nitrodopamine and nitro-DOPA.<sup>63</sup> Catechol groups of nitrodopamine and nitro-DOPA bonded to metal

ions irreversibly and remained stable after several washings at high temperatures.

Rodenstein *et al.* developed a fluorinated nitrodopamine based self-assembly monolayer on titanium oxide to achieve a hydrophobic surface.<sup>64</sup> At first, nitrodopamine hemi-sulfate was synthesized from dopamine *via* nitration with sodium nitrite and sulfuric acid. This was then linked to an activated ester of  $2H,2H,3H,3H$ -perfluoro-undecanoic-acid, *via* amide coupling obtaining perfluoroalkyl nitrodopamine (PFAND) (Scheme 19).

The coating was performed on  $\text{TiO}_2$  through dip coating in a solution of PFAND (2-propanol/water mixture). Interestingly N 1s XPS spectra of PFAND coating showed a splitting of the signal associated with the nitro group. This is explained by the coexistence of two different configurations (Fig. 15). It is hypothesized that the nitro derivative of catechol coordinates with the metal ions *via* two types of binding mode. In bidentate binding both of the two hydroxyl groups dissociates and binds to the metal ion. Whilst in monodentate binding, one hydroxyl group is involved in the hydrogen bond with the oxide surface or adjacent catechol.<sup>60</sup> Another example of nitro-dopamine functional coating was reported by Gomes *et al.*<sup>65</sup> In here, dodecanedioic acid was used as linker between nitro-dopamine and L-homoserine lactone. The obtained product can be considered as an adhesive hybrid of *N*-acyl-L-homoserine lactones (AHLs) which exert antimicrobial activity by interfering with the inter bacterial communication system. This activity, defined as quorum sensing quenching, offers a promising alternative to conventional anti-infective strategies. The localization of these active molecules near the surface by mean of a coating, allowed the preparation of an antibiofilm coating. The synthesis was carried out through sequential substitution of dodecanedioic acid bis-*N*-succinimidyl ester with nitro-dopamine and L-homoserine lactone (Scheme 20). The antibiofilm activity was tested upon coating on  $\text{TiO}_2$  beads. These were



**Scheme 19** Synthesis of nitrodopamine and perfluoroalkyl derivative of nitrodopamine.

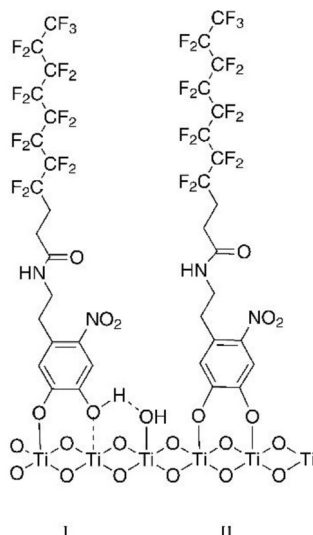
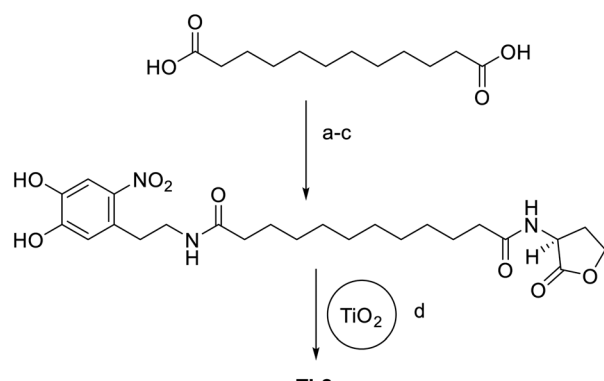


**Fig. 15** Configurations of PFAND adsorption on  $\text{TiO}_2$ . (I) Monodentate binding with a hydrogen bridge to a neighboring surface hydroxide. (II) Bidentate binding, in which both catechol oxygens are deprotonated. Reproduced with permission from ref. 64. Copyright 2010 American Chemical Society.



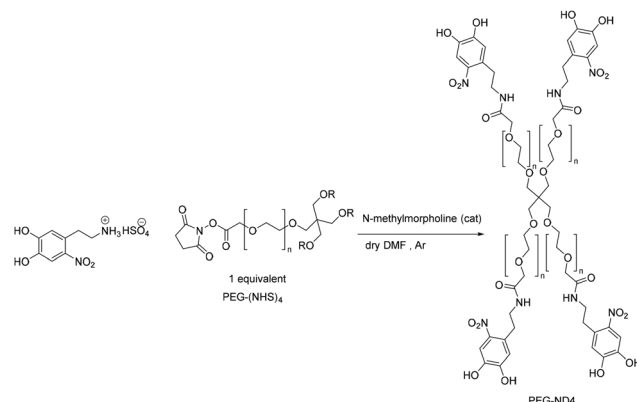
- a)  $N,N'$ -disuccinimidyl carbonate, pyridine, MeCN, rt, 7 h, quant;
- b) nitrodopamine,  $\text{Et}_3\text{N}$ , THF/DMSO, rt, 20 h
- c) L-homoserine lactone,  $\text{Et}_3\text{N}$ , THF/DMSO, rt, 20 h, 72 %
- d) 0.1 M MOPS/ 0.6 M NaCl/ 0.6 M  $\text{K}_2\text{SO}_4$ , 4 h, 50 °C

**Scheme 20** Synthesis and coating formation of L-homoserine lactone-nitrodopamine conjugate.

easily functionalized through simple dip coating MOPS buffer for 4 h at 50 °C.

As final example, Shafiq *et al.* exploited photocleavable nitrocatechol derivatives for on demand debonding of a gel coating.<sup>66</sup> Nitrodopamine was functionalized with a four-arm star-poly(ethyleneglycol) to form PEG-ND4 derivative by reacting with PEG-(NHS)<sub>4</sub> (Scheme 21).

PEG-ND4 crosslinked hydrogel films where formed on quartz substrates either through covalent crosslinking on the surface or  $\text{Fe}^{3+}$ -mediated crosslinking. On demand depolymerization would then be triggered *via* photolytic reaction of the



**Scheme 21** Synthesis of PEG-ND4.

*o*-nitrophenyl ethyl moiety causing the detachment of the catechol units (Fig. 16).

### Caffeic acid derivatives

Caffeic acid, is a naturally occurring phenolic acid and belongs to the broader class of polyphenols.<sup>67</sup> These compounds have been extensively studied for their antioxidant and antimicrobial properties as well as in their use as platforms for drug delivery both in the formation of supramolecular networks and as coatings.<sup>68</sup> Caffeic acid and its derivatives, including dihydrocaffeic acid (DHCA), 3,4-dihydroxyphenylacetic acid (DOPAC), and gallic acid (GA), offer alternative building blocks for the modification of active molecules toward functional coatings (Fig. 17).<sup>53,69,70</sup>

Ahn *et al.* reported the use of dihydrocaffeic acid (DHCA) as starting material for the development of a catechol based zwitter ionic surfactant derivative mimicking mfp interactions responsible for its strong wet adhesive properties.<sup>71</sup> The catecholic zwitter ion was formed by introducing in the structure of DHCA an anionic phosphate/cationic quaternary

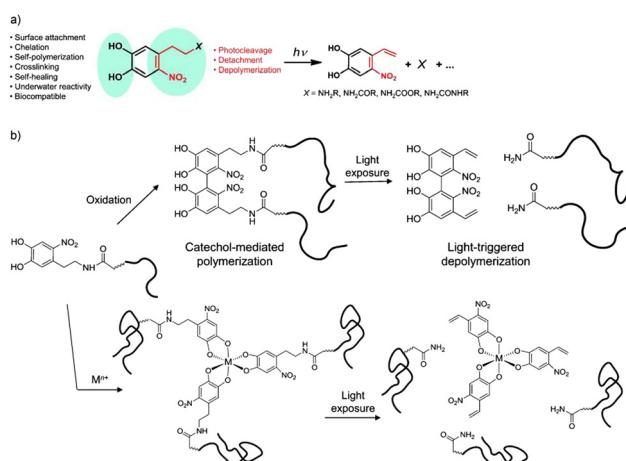


**Fig. 16** Photocleavage of nitrodopamine derivatives. Reproduced with permission from ref. 66. Copyright 2008 John Wiley and Son.



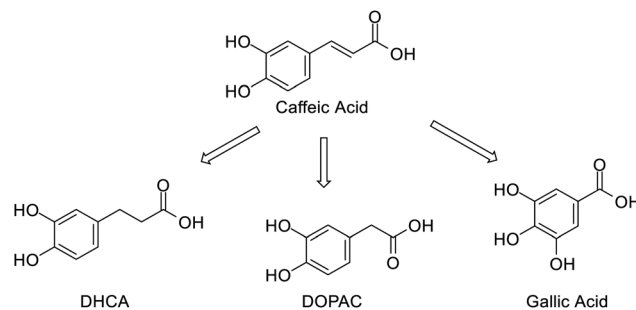


Fig. 17 Derivatives of caffeic acid.

ammonium polar head and an alkyl chain apolar tail. The synthetic procedure involved the protection of catecholic OH with benzyl bromide and reduction with lithium aluminum hydride to the desired alcohol derivative. Then, the zwitter ionic compound (Z-cat-C10) was synthesized *via* Chabrier-reaction, followed by deprotection by hydrogenolysis (Pd/C, H<sub>2</sub>) (Scheme 22).

Upon NaIO<sub>4</sub> mediated oxidation of Z-cat-C10 a thin uniform film (<4 nm) on mica surface, was formed and with an adhesive strength of 50 mJ m<sup>-2</sup>. As shown in Fig. 18, such strong bonding was the result of a combination of hydrophobic interactions of the alkyl side chain and H-bond interaction/covalent crosslinking of the catechol moieties.

Li *et al.* reported the functionalization of titanium implants with caffeic acid–deferoxamine (CA-DFO) conjugate affording enhanced integration of the implant by osteogenesis and angiogenesis.<sup>72</sup> Deferoxamine (DFO) is employed in the treatment of osteonecrosis of the femoral head (ONFH), a complex orthopedic disease. DFO affects biological pathways associated with hypoxia induced factor (HIF), which is involved in angiogenesis and osteointegration. DFO conjugated caffeic acid was synthesized *via* amide bond formation through EDC–HOBT coupling reaction (Scheme 23). CA-DFO was grafted on tita-

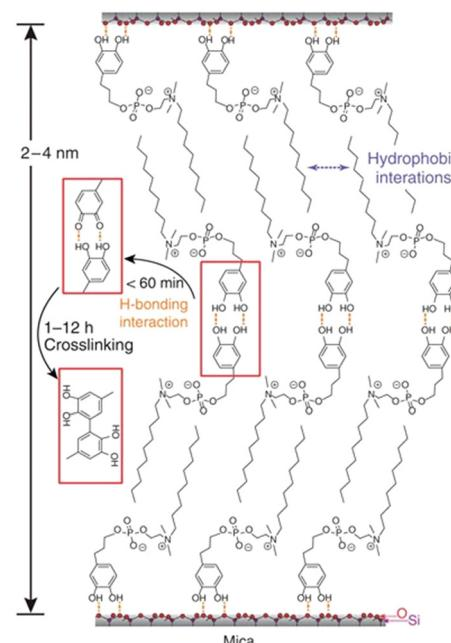
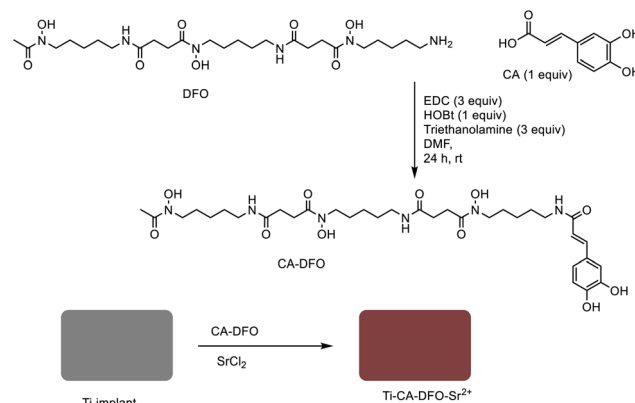
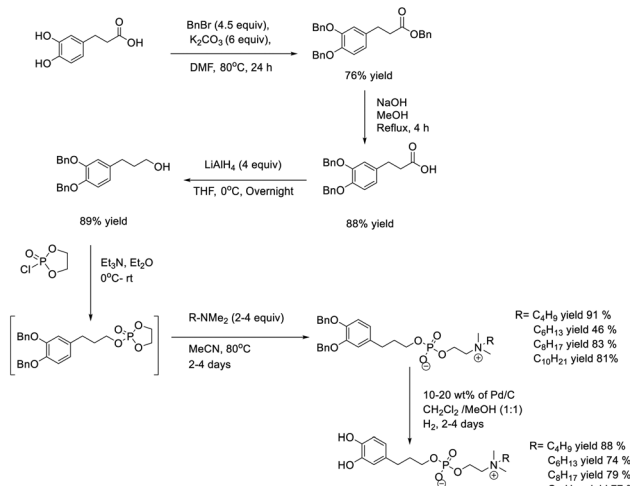


Fig. 18 Graphical representation of the two self-assembled nano-glue layers (upper and lower, respectively) and the interface. Reproduced from ref. 71 under CC BY 4.0 Springer Nature.



Scheme 23 Synthesis of caffeic acid–deferoxamine (CA–DFO) conjugate and polymerization with SrCl<sub>2</sub> on Ti.



Scheme 22 Synthesis of a surfactant zwitterionic complex of catechol.

nium implant in the presence of caffeic acid and strontium chloride dissolved in tris-buffer medium. The catechol ability to chelate metal ions was exploited to incorporate strontium ions (Sr<sup>2+</sup>), which is also associated with osteointegration. This further shows the potential and versatility of catechol coatings in practical applications. Fig. 19 depicts the coordination of Sr<sup>2+</sup> ions from the polymerized CA–DFO conjugate coating on titanium (T-CS-D).

Pozo-Toress *et al.* synthesized exploited caffeic acids derivatives for the development of clickable iron oxide nanoparticles (IONPs) for biomedical applications.<sup>73</sup> Caffeic acid (CA), dihydrocaffeic acid (DHCA) and gallic acid (GA) were first linked to PEG chains carrying an azide group, through esterification,



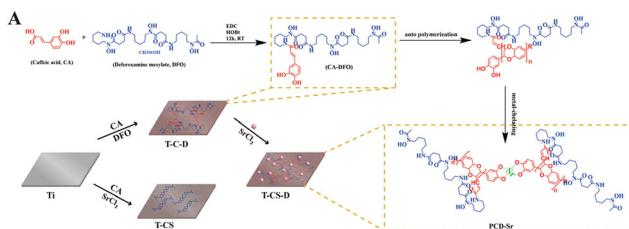
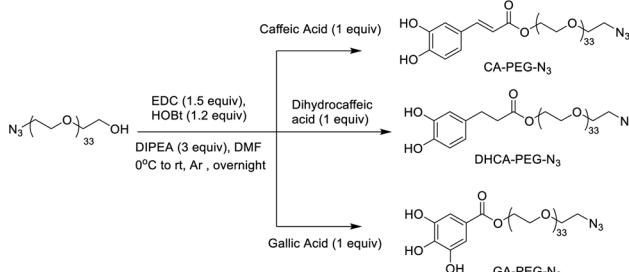


**Fig. 19** Schematic diagram of the chemical synthesis of Ti modified with CA-DFO and Sr<sup>2+</sup>(T-CS-D). Reproduced with permission from ref. 72. Copyright 2023 John Wiley and Son.



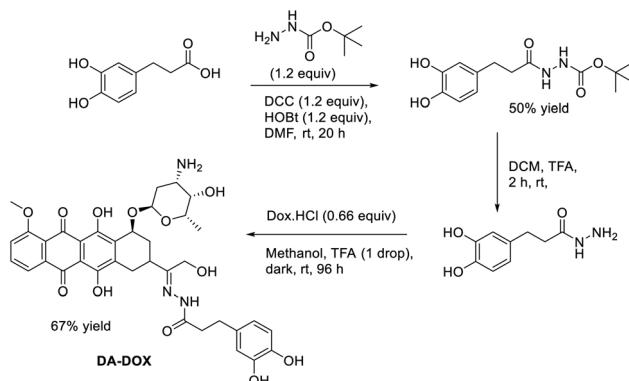
**Scheme 24** Synthesis of caffeic acid derivatives of PEG-azide.

and then anchored onto magnetic nanoparticle (Scheme 24). The conjugation of the carboxylic group with catechol reflected the lower yield of DHCA-PEG-N<sub>3</sub> (38%) compared to the GA and CA analogues (51% and 41% respectively).

Oleic acid capped iron oxide nanoparticles could be easily coated with the bi-functional linkers by displacement of the oil layer. The possibility of incorporating different molecules to the functionalized nanoparticles was further explored by click chemistry.

A similar approach was used by Amstad *et al.* for the preparation of biotin decorated magnetic particles. Gallic acid was coupled, following the same aforementioned conditions, with PEG chains carrying biotin.<sup>74</sup>

Besides surface modification, catechol derivatives can be utilized as bi-functional crosslinkers to functionalize nanoparticles with various drug molecules. Du *et al.* developed a polymer-drug conjugate of dihydrocaffeic acid (DHCA) and doxorubicin (DOX) to deliver DOX to the target site in chemotherapy.<sup>75,76</sup> They demonstrated that the polymer-drug conjugate could be stimulated to release DOX by radiation, showing a synergistic effect with photothermal therapy (PT). The DHCA-doxorubicin conjugate was synthesized *via* a hydrazone bond (Scheme 25) which can be cleaved *via* endosomal pH or NIR irradiation. For the synthesis of the conjugate compound, an amide coupling reaction was done between 3,4-dihydroxy-caffeicacid (DHCA) and monoboc-hydrazine in the presence of HOBT and DCC in DMF. DA-DOX conjugate was then obtained upon Boc removal and reaction with DOX (Scheme 25). Finally, polydopamine doxorubicin conjugate



**Scheme 25** Synthesis of DA-DOX conjugate.

nanoparticles (PDCN) were prepared by polymerizing DA-DOX in the presence of dopamine in tris buffer under air.

Doxorubicin pH-dependent release from PDCN was confirmed studying the behavior of PDCN<sub>25</sub> (25% of DOX compared to PDCN) at pH 7.4, 6.0 and 5.0 respectively in PBS buffer. The percentages of released doxorubicin were 7.9%, 25.4% and 47.2% respectively. Moreover, the release of doxorubicin upon NIR irradiation was almost 2-fold higher, suggesting possible synergistic application in photothermal-chemotherapy (PT-CT) (Fig. 20).

Finally, the same research group also reported the synthesis of polydopamine-chlorambucil conjugate nanoparticles (PDCBs) containing a disulfide linker which could be cleaved by cellular glutathione, pH or NIR irradiation.<sup>76</sup> PDCBs prodrug, dopamine-chlorambucil (DA-CB) conjugate, was synthesized *via* multistep procedure from DHCA. The hydroxyl group of DHCA was protected as a ketal with acetone using phosphorus trichloride (PCl<sub>3</sub>) to afford 2,2-dimethyl-1,3-benzodioxole-5-propanoic acid. 2,2'-Dithiodiethanol was employed as linker with chlorambucil *via* sequential ester bond formation (Scheme 26). Further, PDCBs conjugate nanoparticles were prepared using a similar procedure as for synthesizing PDCN. PDCB nanoparticles showed desirable photo-thermal properties and selective tumor accumulation effect. Intracellular pH, reducing agents and NIR irradiation could influence the drug release profile. Moreover, mild NIR

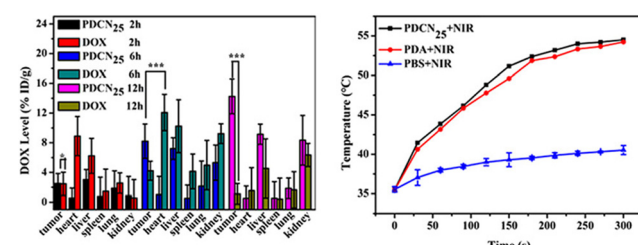
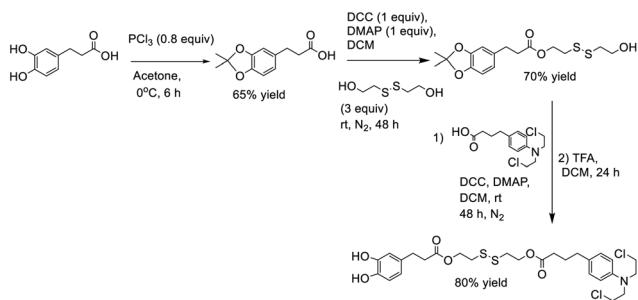


**Fig. 20** Biodistribution of DOX from PDCN<sub>25</sub> in a tumor-bearing mice at different tissues (left). Temperature evolution curve of the tumor site upon the irradiation time (right). Reproduced with permission from ref. 75. Copyright 2017 American Chemical Society.





Scheme 26 Synthesis of dopamine–chlorambucil conjugate.

irradiation sharply enhanced the drug diffusion and showed a faster release profile of 74% in 2 h.

### A critical view on catechol precursors

Although the possible mechanisms behind coating formation *via* dopamine polymerization have been extensively investigated, the debate over the exact composition of polydopamine

is still ongoing. It is suggested that dopamine polymerizes to polydopamine through the auto-oxidation of dopamine to form dopamine orthoquinone, followed by intramolecular cyclization, oxidation, and isomerization. A recent paper from Hemmatpour *et al.* provides an overview of three models depicted based on spectroscopic, mass, and XPS data: (i) polymeric model (ii) physical model (iii) trimer-based model.<sup>25</sup> The polymeric model sees the formation of eumelanin-like structures and polymerization *via* covalent bond formation between the 5,6-dihydroxyindole units. According to the physical model, PDA is considered as a supramolecular aggregate consisting of 5,6-dihydroxyindole and its quinone derivative, held together by hydrogen bonding,  $\pi$ – $\pi$  interactions, and charge transfer interactions. The trimer-based model suggests a complex interplay between dopamine chromes and dopamine oligomers as the major components of the PDA structure. Based on these models, 5,6-dihydroxyindole (5,6-DHI) is a key unit in dopamine polymerization. However, it is not essential for coating formation. In a report from Alfieri *et al.* the sole use 5,6-DHI, under conventional PDA coating conditions (pH 8.5, Tris buffer), could not afford the formation of

Table 1 Summary of catechol direct modification functional coatings

Catechol source	Target compound	Protection strategy	Materials	Application	Ref.
Levodopa	N-Methoxyethyl glycine peptoid, sarcosine peptoid	Acetonide protection on hydroxyl group, Boc <sub>2</sub> O	TiO <sub>2</sub>	Antifouling, antibacterial	21 and 22
	Sulfobetaine methacrylate	Acetonide protection on hydroxyl group, Boc <sub>2</sub> O	Metal (TiO <sub>2</sub> , Au), glass (SiO <sub>2</sub> ), plastic (PC, PE, PU and PTFE)	Antifouling	23
	Polyethylene glycol (m-PEG)	Borate buffer	TiO <sub>2</sub>	Antifouling	26 and 27
	Hexaethylene glycol (EG6)	TBDMS, Boc <sub>2</sub> O	TiO <sub>2</sub>	Antibacterial	28
	TEMPO	TBDMS, Boc <sub>2</sub> O	Hydroxyapatite	Bacterial biofilm inhibition	29
	Sulfobetaine zwitter ion	TBDMS, Boc <sub>2</sub> O	TiO <sub>2</sub> , stainless steel, and nylon	Antifouling and antibacterial	31
	Carboxybetaine zwitter ion	TBDMS, Boc <sub>2</sub> O	Gold, Ti/TiO <sub>2</sub> , SS, PTFE, and PU	Antifouling	30
	Tetrazine complex	Boc <sub>2</sub> O	Polypropylene, PET	Multifunctional surface <i>via</i> Tet-TCO ligation	33
	Azide/alkyne	Borax	Iron oxide nanoparticles, titanium	Clickable surface	43 and 44
	Hyperbranched polyglycol		Metal (TiO <sub>2</sub> , aluminum), SiO <sub>2</sub> , glass, and plastics (PS, PP)	Antifouling surface	46
Anachelin Nitrodopamine	Sulfobetaine		TiO <sub>2</sub> , nitinol alloy	Antifouling, antibacterial	48
	m-PEG, vancomycin		TiO <sub>2</sub>	Antibacterial	56
	Perfluoroalkyl derivative		TiO <sub>2</sub>	Hydrophobic surface	64
	m-PEG		Iron oxide nanoparticles (NPs)	Stabilization of NPs for MRI	61 and 74
Caffeic acid/ dihydrocaffeic acid	N-Acyl-L-homoserine lactone (AHL)		TiO <sub>2</sub>	Antibiofilm coating	65
	m-PEG			Stable gel, light-triggered debonding and degradation	66
	Zwitter ion	Benzyl protection	Mica surface	Strong wet adhesive	71
	Deferoxamine		Titanium	To promote osteogenesis	72
	PEG-azide		Iron oxide nanoparticles	Functionalization <i>via</i> click chemistry	73
	Doxorubicin			pH or NIR trigger drug release	75
	Chlorambucil			Drug delivery	76



a coating on glass samples. The role of primary amino groups in catechol polymerization has been well-established since its inception. This was recognized in the adhesive mussels' foot protein and inspired Messersmith's work on dopamine. In 2014, Wang *et al.* reported the use of catechol and polyamines to modify polypropylene separators in lithium-ion batteries with the formation of PDA-like coatings.<sup>77</sup> In 2016, Hu and colleagues investigated the polymerization of various dopamine analogues with different alkyl chain lengths between the amine and catechol to understand the role of cyclic intermediates PDA synthesis.<sup>78</sup> They concluded that covalent linkage *via* an alkyl chain between catechol and amine is not necessary for polymerization. Co-deposition of catechol and alkylamines in basic conditions could also result in polymerize, but without coating formation on PTEE. García *et al.* demonstrated that the co-deposition of pyrocatechol and hexamethylenediamine in a carbonate buffer solution at pH 9.1 can form a coating on various substrates, including glass, gold, silicon, and fabric.<sup>79</sup> These data suggest that a catechol must be combined with an alkylamine *via* a covalent bond to achieve best coating properties. This result is reflected in Table 1, which compares the coating ability of various catechol precursors on different substrates. The table shows that levodopa conjugates can coat most substrates (metal, glass, and plastic), whereas dopamine and caffeic acid derivatives can only coat metals and metal oxides. It is important to note that levodopa contains a free primary amine that behaves similarly to the one in free dopamine. However, upon preparation of the corresponding derivatives, the amino group is involved in an amide bond, in the case of dopamine, whilst remains free when levodopa is coupled *via* the carboxylic group. Conjugates of dopamine and caffeic acid do not form the same intermediate discussed in PDA synthesis and appear to form coatings mainly on metals and metal oxides *via* coordination bond formation between the metal ion and the hydroxyl group of catechol. On the other hand levodopa seems to be more versatile and material agnostic allowing also for coatings on plastics and fabrics. However, the synthesis of levodopa conjugates is more laborious as protection of the amino group is required for further functionalization. Conversely, the synthesis of dopamine and caffeic acid conjugates does not require protection/deprotection steps. Moreover, in the case of polymers modified with multiple catechol groups polymerization of the latter becomes irrelevant. In addition, the literature suggests that the coating ability can be improved upon reaction of the catechol residue with amino groups, either *via* intra or intermolecular pathway. Nonetheless, this aspect remains underexplored by the available literature.

In conclusion, the choice of catechol precursor is mainly guided by the material of targeted substrate, the functional molecule and its compatibility with the coupling chemistry.

## Conclusions

In this review, we have summarized the development of surface functionalization techniques through direct modifi-

cation with catechol derivatives. Several synthetic routes were described to offer a wide range of possibilities depending on the catechol derivative and the coupling chemistry. This would allow the reader for a better choice of the reaction conditions in terms of selectivity and yield. Moreover, reports covering various practical applications and substrate materials were included. Nonetheless, proper comparison among different approaches was not possible due to inconsistencies regarding substrate materials and surface characterization techniques. Although direct modification is a robust strategy for the modification of surfaces *via* simple dip coating, it is also associated with some shortcomings such as coating stability and coating time. Most reports on catechol-based surface modification techniques use multi-step bottom-up approaches, whilst catechol bearing molecules, obtained through direct modification, can be coated on the desired surface in a single step. Nonetheless, several reports describe lengthy coating protocols (12–24 h), which might limit its implementation (*e.g.* point of care medical devices functionalization). In this frame, electrochemical deposition and oxidant promoted polymerization could represent valuable alternatives to conventional dip coating. Cathodic deposition and polymerization of dopamine has been reported as a reliable and effective methodology.<sup>80</sup> As the oxidation of the catechol moieties is driven by the application of an electric potential at the electrode, the reaction can happen also at low pH values at which spontaneous PDA formation cannot occur. As a result, greater control on coating thickness and homogeneity can be achieved as the reaction happens solely at the electrode surface and is governed by the potential applied. Moreover, since polymerization in the bulk of the solution is inhibited, waste production can be significantly reduced. Nonetheless, this approach is only applicable to conductive substrates. On the other hand, oxidants as ammonium persulfate<sup>81</sup> or sodium periodate<sup>82</sup> have been successfully for the rapid preparation of films on a variety of substrates while reducing the coating time to a few hours or even minutes in the case of sodium periodate. These conditions are applicable to spray coating which is particularly suited for on-site applications or for the treatment of wide surfaces. Also in this case, the oxidation-polymerization cascade happens in a wider pH window.<sup>83</sup> Wider application of these coating conditions to catechol conjugates could drastically increase their translational potential and meet practical requirements in terms of speed and reproducibility.

The formation of a covalent bond between the adhesive moiety and the active molecules is advantageous as it increases stability and prevents loss of function due to leaching. Moreover, higher loading could be obtained with direct modification compared to multi step bottom-up functionalization. Mechanical strength and stability of the obtained coatings requires further investigation as catechol derivatives often produce monolayer films with less performing mechanical properties than polydopamine. Finally, aspects as loading capacity, durability, cost and environmental sustainability should be further emphasized in the optimization of the coating conditions. This would allow for better comparison



among different synthetic approaches, especially while targeting the requirements for industrial or large-scale applications.

## Author contributions

B. M. writing and editing, E. V. V. d. E. writing, review and editing, G. A. C. conceptualization, writing, review and editing.

## Conflicts of interest

The authors declare no conflict of interest.

## Data availability

No data was used for the research described in the article.

## Acknowledgements

This publication was funded by the European Union through the Horizon Europe Framework Program (HORIZON) under grant number 101057992 (Recipients BM, writing; EVVdE, writing and revision). This publication has been prepared with the support of the “RUDN University Strategic Academic Leadership Program” (recipient EVVdE, writing and revision).

## References

- Q. Ye, F. Zhou and W. Liu, *Chem. Soc. Rev.*, 2011, **40**, 4244–4258.
- E. Faure, C. Falentin-Daudré, C. Jérôme, J. Lyskawa, D. Fournier, P. Woisel and C. Detrembleur, *Prog. Polym. Sci.*, 2013, **38**, 236–270.
- H. Lee, S. M. Dellatore, W. M. Miller and P. B. Messersmith, *Science*, 2007, **318**, 426–430.
- H. G. Silverman and F. F. Roberto, *Mar. Biotechnol.*, 2007, **9**, 661–681.
- H. Lee, N. F. Scherer and P. B. Messersmith, *Proc. Natl. Acad. Sci. U. S. A.*, 2006, **103**, 12999–13003.
- J. H. Waite and M. L. Tanzer, *Science*, 1981, **212**, 1038–1040.
- J. H. Waite and X. Qin, *Biochemistry*, 2001, **40**, 2887–2893.
- V. V. Papov, T. V. Diamond, K. Biemann and J. H. Waite, *J. Biol. Chem.*, 1995, **270**, 20183–20192.
- J. H. Waite, *Ann. N. Y. Acad. Sci.*, 1999, **875**, 301–309.
- D. J. Crisp, G. Walker, G. A. Young and A. B. Yule, *J. Colloid Interface Sci.*, 1985, **104**, 40–50.
- J. H. Waite, *Integr. Comp. Biol.*, 2002, **42**, 1172–1180.
- M. L. Alfieri, L. Panzella and A. Napolitano, *Eur. J. Org. Chem.*, 2024, e202301002.
- P. Yang, F. Zhu, Z. Zhang, Y. Cheng, Z. Wang and Y. Li, *Chem. Soc. Rev.*, 2021, **50**, 8319–8343.
- J. Yang, M. A. Cohen Stuart and M. Kamperman, *Chem. Soc. Rev.*, 2014, **43**, 8271–8298.
- A. B. Asha, Y. Chen and R. Narain, *Chem. Soc. Rev.*, 2021, **50**, 11668–11683.
- C. Zhang, B. Wu, Y. Zhou, F. Zhou, W. Liu and Z. Wang, *Chem. Soc. Rev.*, 2020, **49**, 3605–3637.
- M. Sugumaran and J. J. Evans, *J. Funct. Biomater.*, 2023, **14**(9), 449.
- M. Yu and T. J. Deming, *Macromolecules*, 1998, **31**, 4739–4745.
- B.-H. Hu and P. B. Messersmith, *Tetrahedron Lett.*, 2000, **41**, 5795–5798.
- Z. Liu, B.-H. Hu and P. B. Messersmith, *Tetrahedron Lett.*, 2008, **49**, 5519–5521.
- A. R. Statz, R. J. Meagher, A. E. Barron and P. B. Messersmith, *J. Am. Chem. Soc.*, 2005, **127**, 7972–7973.
- K. H. A. Lau, C. Ren, T. S. Sileika, S. H. Park, I. Szleifer and P. B. Messersmith, *Langmuir*, 2012, **28**, 16099–16107.
- J. Kuang and P. B. Messersmith, *Langmuir*, 2012, **28**, 7258–7266.
- M. J. Sever and J. J. Wilker, *Tetrahedron*, 2001, **57**, 6139–6146.
- H. Hemmatpour, O. De Luca, D. Crestani, M. C. A. Stuart, A. Lasorsa, P. C. A. van der Wel, K. Loos, T. Giousis, V. Haddadi-Asl and P. Rudolf, *Nat. Commun.*, 2023, **14**, 664.
- J. L. Dalsin, B.-H. Hu, B. P. Lee and P. B. Messersmith, *J. Am. Chem. Soc.*, 2003, **125**, 4253–4258.
- J. L. Dalsin, L. Lin, S. Tosatti, J. Vörös, M. Textor and P. B. Messersmith, *Langmuir*, 2005, **21**, 640–646.
- S. H. Ki, S. Lee, D. Kim, S. J. Song, S.-P. Hong, S. Cho, S. M. Kang, J. S. Choi and W. K. Cho, *Langmuir*, 2019, **35**, 14465–14472.
- H. Woehlk, M. J. Trimble, S. C. Mansour, D. Pletzer, V. Trouillet, A. Welle, L. Barner, R. E. W. Hancock, C. Barner-Kowollik and K. E. Fairfull-Smith, *Polym. Chem.*, 2019, **10**, 4252–4258.
- I. Han, S. Y. Kim, S.-P. Hong, I. S. Choi and W. K. Cho, *Prog. Org. Coat.*, 2023, **184**, 107860.
- D. K. Yeon, S. Ko, S. Jeong, S.-P. Hong, S. M. Kang and W. K. Cho, *Langmuir*, 2019, **35**, 1227–1234.
- R. Ukita, K. Wu, X. Lin, N. M. Carleton, N. Naito, A. Lai, C. C. Do-Nguyen, C. T. Demarest, S. Jiang and K. E. Cook, *Acta Biomater.*, 2019, **92**, 71–81.
- K. Hast, M. R. L. Stone, Z. Jia, M. Baci, T. Aggarwal and E. C. Izgu, *ACS Appl. Mater. Interfaces*, 2023, **15**, 4996–5009.
- H. A. Lee, Y. Ma, F. Zhou, S. Hong and H. Lee, *Acc. Chem. Res.*, 2019, **52**, 704–713.
- X. Fan, L. Lin, J. L. Dalsin and P. B. Messersmith, *J. Am. Chem. Soc.*, 2005, **127**, 15843–15847.
- H. Lee, B. P. Lee and P. B. Messersmith, *Nature*, 2007, **448**, 338–341.
- P. Glass, H. Chung, N. R. Washburn and M. Sitti, *Langmuir*, 2009, **25**, 6607–6612.
- X. Wang, Q. Ye, T. Gao, J. Liu and F. Zhou, *Langmuir*, 2012, **28**, 2574–2581.



39 M. Kohri, S. Yamazaki, S. Irie, N. Teramoto, T. Taniguchi and K. Kishikawa, *ACS Omega*, 2018, **3**, 16626–16632.

40 A. Schneider, J. Hemmerlé, M. Allais, J. Didierjean, M. Michel, M. d'Ischia and V. Ball, *ACS Appl. Mater. Interfaces*, 2018, **10**, 7574–7580.

41 J. M. Belitsky, *Bioorg. Med. Chem. Lett.*, 2010, **20**, 4475–4478.

42 J. Szewczyk, V. Babacic, A. Krysztofik, O. Ivashchenko, M. Pochylski, R. Pietrzak, J. Gapiński, B. Graczykowski, M. Bechelany and E. Coy, *ACS Appl. Mater. Interfaces*, 2023, **15**, 36922–36935.

43 A. S. Goldmann, C. Schödel, A. Walther, J. Yuan, K. Loos and A. H. E. Müller, *Macromol. Rapid Commun.*, 2010, **31**, 1608–1615.

44 M. A. Watson, J. Lyskawa, C. Zobrist, D. Fournier, M. Jimenez, M. Traisnel, L. Gengembre and P. Woisel, *Langmuir*, 2010, **26**, 15920–15924.

45 A. A. Putnam and J. J. Wilker, *Soft Matter*, 2021, **17**, 1999–2009.

46 Q. Wei, T. Becherer, R.-C. Mutihac, P.-L. M. Noeske, F. Paulus, R. Haag and I. Grunwald, *Biomacromolecules*, 2014, **15**, 3061–3071.

47 C.-J. Huang, L.-C. Wang, J.-J. Shyue and Y.-C. Chang, *Langmuir*, 2014, **30**, 12638–12646.

48 H. L. Bui, S.-D. Huang, B. P. Lee, M.-Y. Lan and C.-J. Huang, *Colloids Surf. B*, 2022, **220**, 112879.

49 L. Q. Xu, D. Pranantyo, K.-G. Neoh, E.-T. Kang, S. L.-M. Teo and G. D. Fu, *Polym. Chem.*, 2016, **7**, 493–501.

50 M. J. McWhirter, P. J. Bremer, I. L. Lamont and A. J. McQuillan, *Langmuir*, 2003, **19**, 3575–3577.

51 K. Gademann, *ChemBioChem*, 2005, **6**, 913–919.

52 K. Gademann, Y. Bethuel, H. H. Locher and C. Hubschwerlen, *J. Org. Chem.*, 2007, **72**, 8361–8370.

53 K. Gademann, J. Kobylinska, J.-Y. Wach and T. M. Woods, *BioMetals*, 2009, **22**, 595–604.

54 S. Zürcher, D. Wäckerlin, Y. Bethuel, B. Malisova, M. Textor, S. Tosatti and K. Gademann, *J. Am. Chem. Soc.*, 2006, **128**, 1064–1065.

55 J.-Y. Wach, B. Malisova, S. Bonazzi, S. Tosatti, M. Textor, S. Zürcher and K. Gademann, *Chem. – Eur. J.*, 2008, **14**, 10579–10584.

56 J.-Y. Wach, S. Bonazzi and K. Gademann, *Angew. Chem., Int. Ed.*, 2008, **47**, 7123–7126.

57 A. Avdeef, S. R. Sofen, T. L. Bregante and K. N. Raymond, *J. Am. Chem. Soc.*, 1978, **100**, 5362–5370.

58 C. J. Sun, A. Srivastava, J. R. Reifert and J. H. Waite, *J. Adhes.*, 2009, **85**, 126–138.

59 V. M. Nurchi, T. Pivetta, J. I. Lachowicz and G. Crisponi, *J. Inorg. Biochem.*, 2009, **103**, 227–236.

60 B. Malisova, S. Tosatti, M. Textor, K. Gademann and S. Zürcher, *Langmuir*, 2010, **26**, 4018–4026.

61 M. Cenceer, M. Murley, Y. Liu and B. P. Lee, *Biomacromolecules*, 2015, **16**, 404–410.

62 A. Napolitano, A. Palumbo and M. d'Ischia, *Tetrahedron*, 2000, **56**, 5941–5945.

63 E. Amstad, T. Gillich, I. Bilecka, M. Textor and E. Reimhult, *Nano Lett.*, 2009, **9**, 4042–4048.

64 M. Rodenstein, S. Zürcher, S. G. P. Tosatti and N. D. Spencer, *Langmuir*, 2010, **26**, 16211–16220.

65 J. Gomes, A. Grunau, A. K. Lawrence, L. Eberl and K. Gademann, *Chem. Commun.*, 2013, **49**, 155–157.

66 Z. Shafiq, J. Cui, L. Pastor-Pérez, V. San Miguel, R. A. Gropeanu, C. Serrano and A. del Campo, *Angew. Chem., Int. Ed.*, 2012, **51**, 4332–4335.

67 L. Xu, D. Pranantyo, K.-G. Neoh and E.-T. Kang, *ACS Sustainable Chem. Eng.*, 2017, **5**, 3055–3062.

68 X. Gao, Z. Xu, G. Liu and J. Wu, *Acta Biomater.*, 2021, **119**, 57–74.

69 H. Wei, N. Insin, J. Lee, H.-S. Han, J. M. Cordero, W. Liu and M. G. Bawendi, *Nano Lett.*, 2012, **12**, 22–25.

70 A. R. Studart, E. Amstad and L. J. Gauckler, *Langmuir*, 2007, **23**, 1081–1090.

71 B. K. Ahn, S. Das, R. Linstadt, Y. Kaufman, N. R. Martinez-Rodriguez, R. Mirshafian, E. Kesselman, Y. Talmon, B. H. Lipshutz, J. N. Israelachvili and J. H. Waite, *Nat. Commun.*, 2015, **6**, 8663.

72 D. Li, D. Wang, Y. Yang, P. Gao, W. Fan, X. Zhang, Y. Tang, W. Yang and K. Cai, *Adv. Funct. Mater.*, 2023, **33**, 2212016.

73 E. Pozo-Torres, C. Caro, A. Avasthi, J. M. Páez-Muñoz, M. L. García-Martín, I. Fernández and M. Pernia Leal, *Soft Matter*, 2020, **16**, 3257–3266.

74 E. Amstad, S. Zürcher, A. Mashaghi, J. Y. Wong, M. Textor and E. Reimhult, *Small*, 2009, **5**, 1334–1342.

75 C. Du, J. Qian, L. Zhou, Y. Su, R. Zhang and C.-M. Dong, *ACS Appl. Mater. Interfaces*, 2017, **9**, 31576–31588.

76 C. Du, Y. Ding, J. Qian, R. Zhang and C.-M. Dong, *J. Mater. Chem. B*, 2019, **7**, 415–432.

77 H. Wang, J. Wu, C. Cai, J. Guo, H. Fan, C. Zhu, H. Dong, N. Zhao and J. Xu, *ACS Appl. Mater. Interfaces*, 2014, **6**, 5602–5608.

78 H. Hu, J. C. Dyke, B. A. Bowman, C.-C. Ko and W. You, *Langmuir*, 2016, **32**, 9873–9882.

79 S. Suárez-García, J. Sedó, J. Saiz-Poseu and D. Ruiz-Molina, *Biomimetics*, 2017, **2**, 22.

80 S. Kim, L. K. Jang, H. S. Park and J. Y. Lee, *Sci. Rep.*, 2016, **6**, 30475.

81 Q. Wei, F. Zhang, J. Li, B. Li and C. Zhao, *Polym. Chem.*, 2010, **1**, 1430.

82 S. H. Hong, S. Hong, M.-H. Ryou, J. W. Choi, S. M. Kang and H. Lee, *Adv. Mater. Interfaces*, 2016, **3**, 1500857.

83 M. Salomäki, L. Marttila, H. Kivelä, T. Ouvinen and J. Lukkari, *J. Phys. Chem. B*, 2018, **122**, 6314–6327.